YMTHE, Volume *25*

Supplemental Information

A Synthetic Mammalian Therapeutic Gene Circuit for Sensing and Suppressing Inflammation

Anže Smole, Duško Lainšček, Urban Bezeljak, Simon Horvat, and Roman Jerala

SUPPLEMENTARY FIGURES

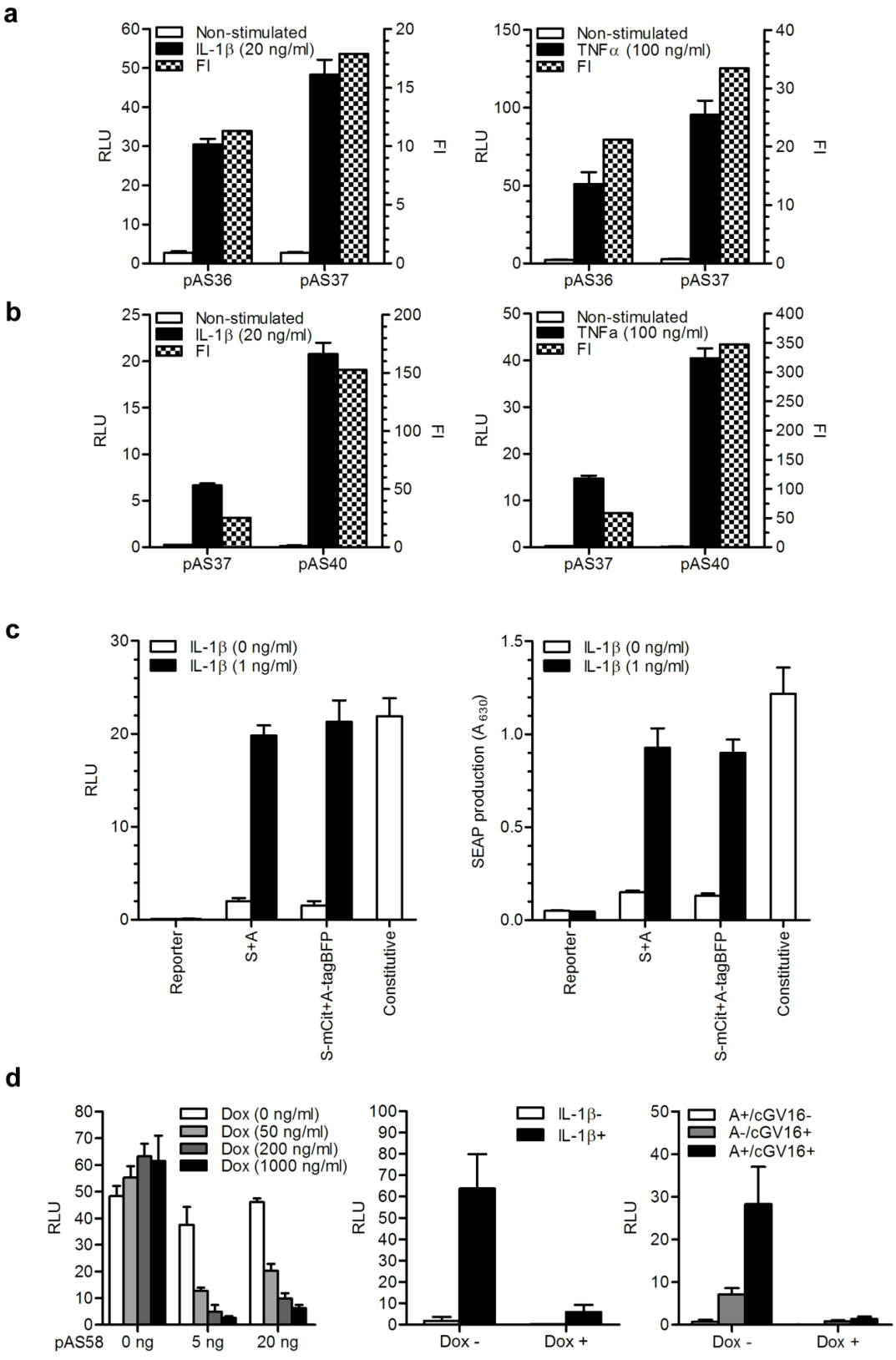

Supplementary Figure 1 Related to Figure 2

Tuning the elements used for constructing the anti-inflammatory device

(**a**) Optimization of NF-κB responsive element. HEK 293T cells were transfected with pAS36 or pAS37 and stimulated with 20 ng/mL IL-1β (left) or 100 ng/mL TNFα (right). After 24 h luciferase activity was measured by dual luciferase test.

(**b**) Optimization of a minimal promoter. HEK 293T cells were transfected with pAS37 or pAS40 and stimulated with 20 ng/mL IL-1β (left) or 100 ng/mL TNFα (right). After 24 h luciferase activity was measured by dual luciferase test.

(**c**) The capacity of system activation. Activated anti-inflammatory device supports comparable reporter expression level to the constitutively expressed control (pAS108; P_{CMV}-Luc or pAS109; P_{CMV}-SEAP) as measured by luciferase (left) or SEAP (right). Similarly, sensor and amplifier constructs with 2A peptide-fluorescent protein fusions (pAS97; TRE-$P_{NF\text{-}κB2}$-P_{MIN}-GV16-myc-2A-mCit and pAS98; TRE-UAS-P_{MIN}-GV16-myc-2A-tagBFP) support comparable system activation to the basic sensor and amplifier. For detailed information about transfected plasmids and their amounts in each specific experiment, see Supplementary table 1 and 2, respectively. Error bars indicate s.d. (*n*=4).

(**d**) Validation of the rtTR-KRAB reset repressor. The constitutively expressed rtTR-KRAB (pAS58; P_{hCMV}-rtTR-NLS-KRAB) represses Gal4-VP16 (plasmid pSGVP)-induced activation of the reporter construct (pAS51; TRE-UAS-P_{MIN}-Luc) in the presence of the increasing concentrations of doxycycline (Dox). In the absence of Dox, pAS58 alone did not significantly influence system activation (left). Activated sensor (middle) and amplifier (right) can also be shut down efficiently.

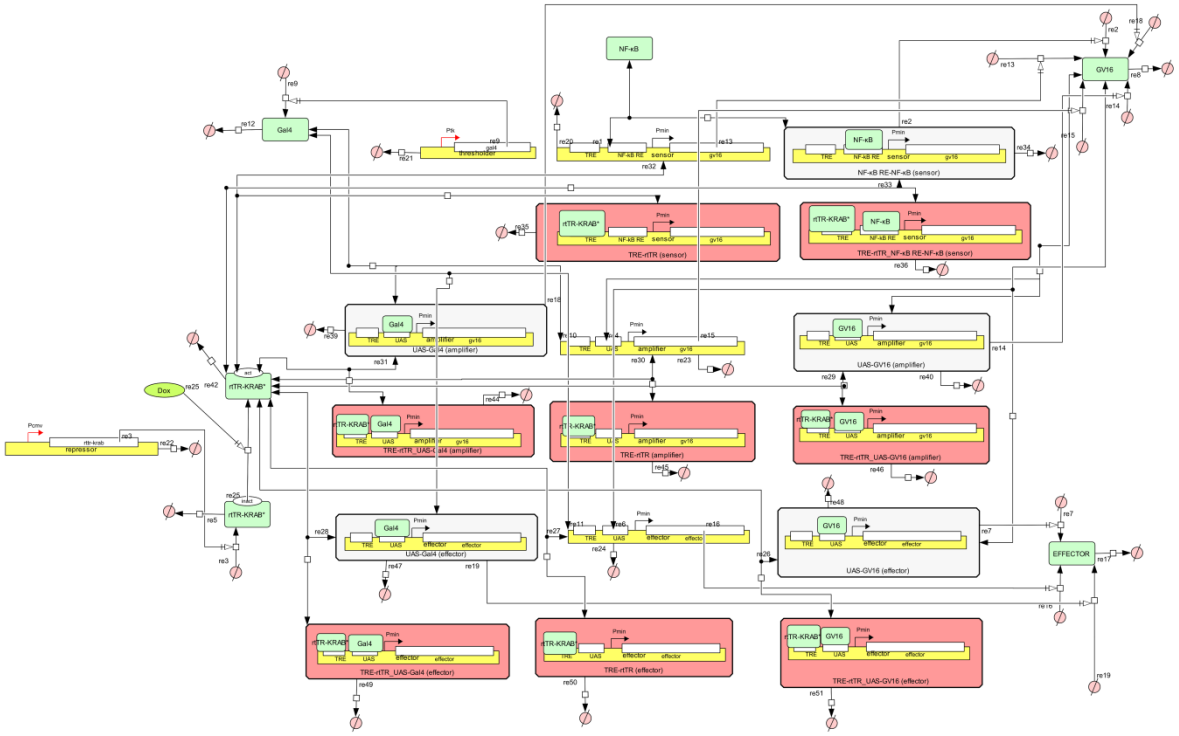

Supplementary Figure 2 Related to the Matematical ODE model

State transition diagram of the genetic circuit.

The state transition diagram of the genetic circuit was constructed using CellDesigner 4.4 software[13]. The state transitions were described with reactions listed in Supplementary Table 5.

a

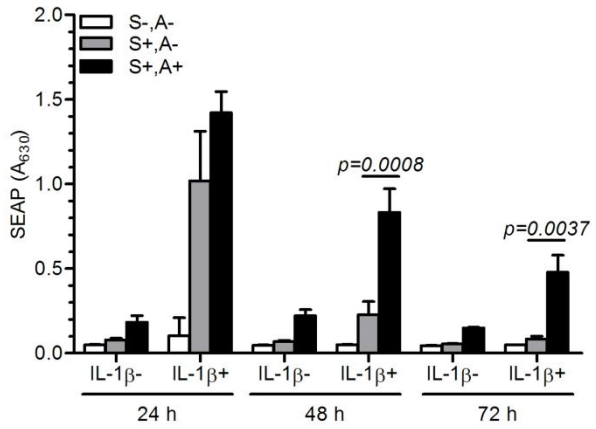
S-,A-
S+,A-
S+,A+
SEAP (A_{630})
2.0
1.5
1.0
0.5
0.0
p=0.0008
p=0.0037
IL-1β-
IL-1β+
IL-1β-
IL-1β+
IL-1β-
IL-1β+
24 h
48 h
72 h

b

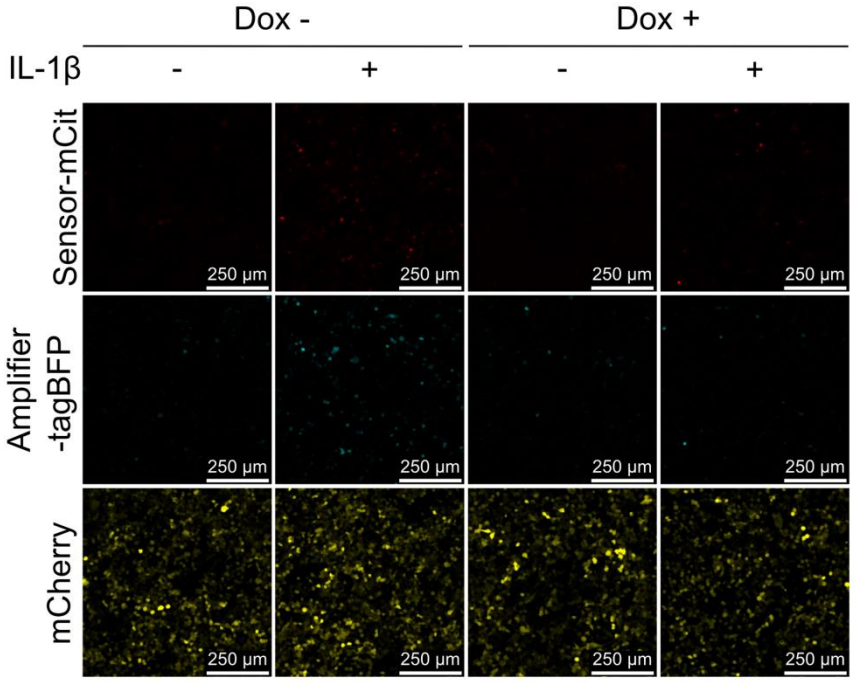
Dox -
Dox +
IL-1β
-
+
-
+
Sensor-mCit
Amplifier -tagBFP
mCherry
250 µm

c

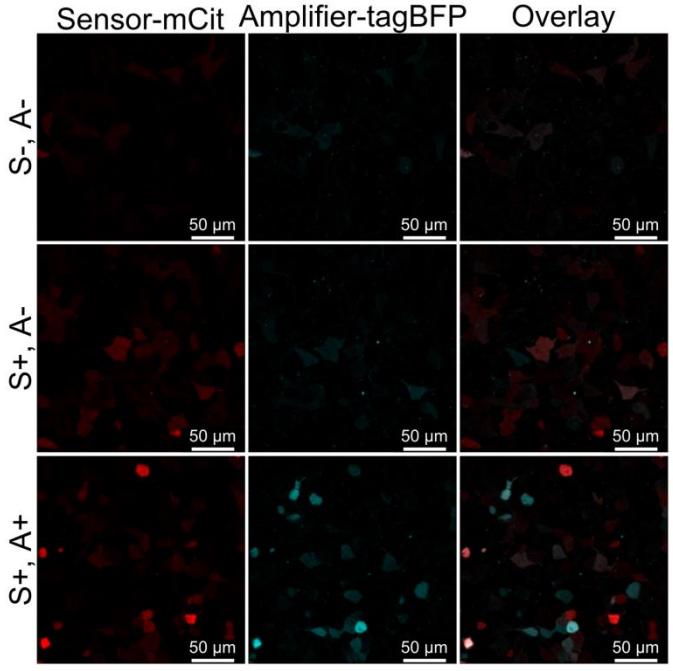
Sensor-mCit
Amplifier-tagBFP
Overlay
S-, A-
S+, A-
S+, A+
50 µm

Supplementary Figure 3 Related to Figure 3

(**a**) Anti-inflammatory device-engineered HEK 293T cells (reporter pAS72; TRE-UAS-P_{MIN}-SEAP) were stimulated with hIL-1β for 4 h and then input signal was removed by medium exchange. SEAP production was quantified in the culture supernatants every 24 h along with a medium exchange to observe kinetics of a system activation. Compared to sensor alone (grey bars), setup which included also amplifier construct (black bars) yielded stronger system activation at the later time points indicating its role in the sustained system activation. For detailed information about transfected plasmids and their amounts in each specific experiment, see the Tables S1 and S2, respectively. Error bars indicate s.d. (*n*=4).

(**b**) Demonstration of the system performance by a confocal fluorescence microscopy of anti-inflammatory device-engineered HEK 293T cells. Sensor and amplifier constructs were observed directly by in frame fusion via 2A peptide with mCitrine and tagBFP reporter genes, respectively (pAS97; TRE-$P_{NF\text{-}\kappa B2}$-P_{MIN}-GV16-myc-2A-mCit and pAS98; TRE-UAS-P_{MIN}-GV16-myc-2A-tagBFP). Twenty-four hours after stimulation, mCitrine and tagBFP positive cells were observed only in the presence of interleukin-1β (IL-1β) and absence of doxycycline (Dox). mCherry was used as a transfection control.

(**c**) System functionality is dependent on intracellular Gal4-VP16 transcriptional activator (GV16) meaning it is inevitable that sensor and enhancer are activated in the same cell. Cells were stimulated with IL-1β for 24 h and then observed by a confocal fluorescence microscopy to demonstrate the simultaneous activation of both constructs in the same cell. For detailed information about transfected plasmids and their amounts in each specific experiment, see the Supplementary Table 1 and 2, respectively. Error bars indicate s.d. (*n*=4).

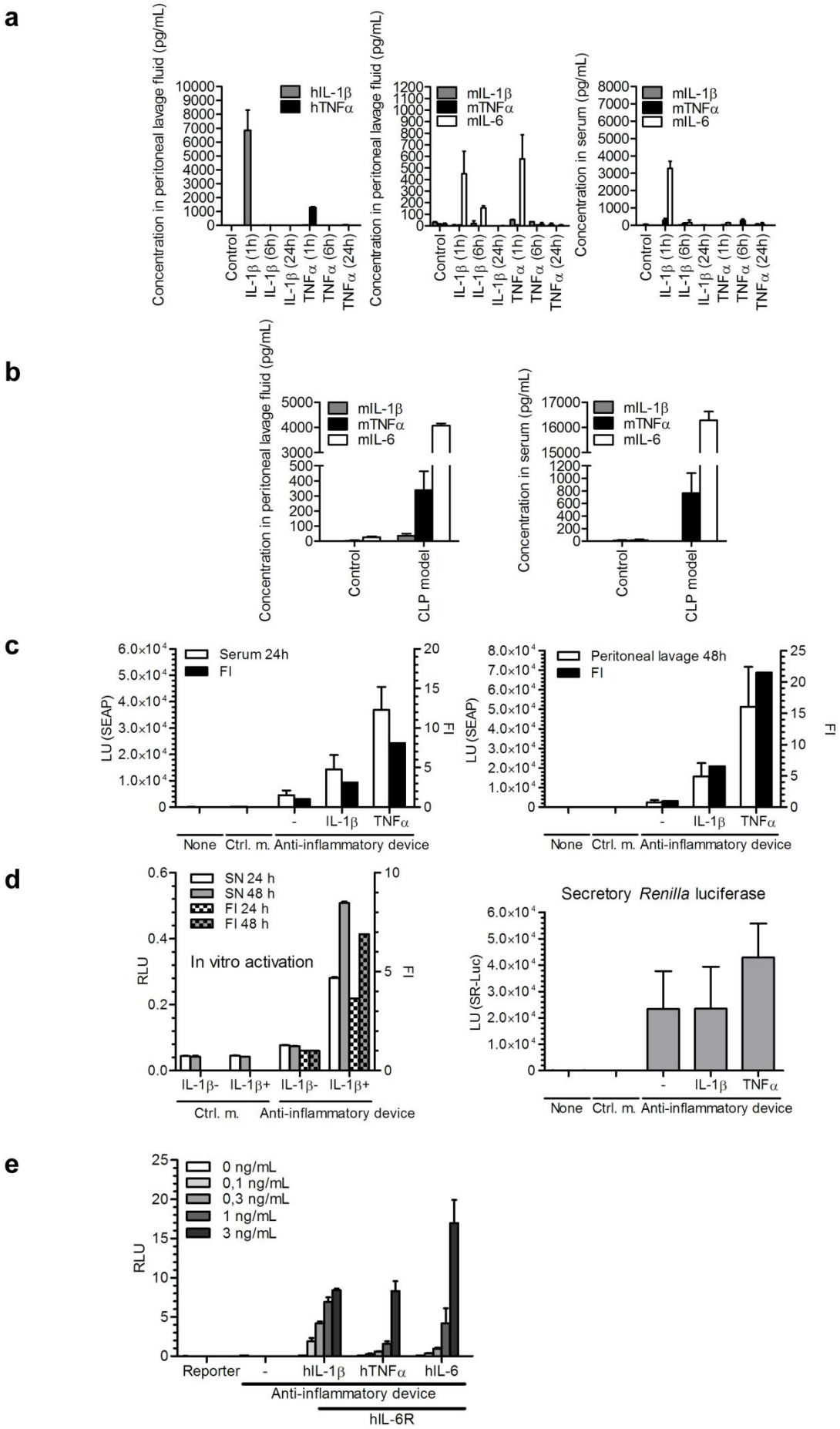
a
Concentration in peritoneal lavage fluid (pg/mL)
hIL-1β
hTNFα
Control
IL-1β (1h)
IL-1β (6h)
IL-1β (24h)
TNFα (1h)
TNFα (6h)
TNFα (24h)
Concentration in peritoneal lavage fluid (pg/mL)
mIL-1β
mTNFα
mIL-6
Concentration in serum (pg/mL)
b
Concentration in peritoneal lavage fluid (pg/mL)
Concentration in serum (pg/mL)
Control
CLP model
c
Serum 24h
FI
LU (SEAP)
Peritoneal lavage 48h
None
Ctrl. m.
Anti-inflammatory device
-
IL-1β
TNFα
d
SN 24 h
SN 48 h
FI 24 h
FI 48 h
In vitro activation
RLU
IL-1β-
IL-1β+
Secretory Renilla luciferase
LU (SR-Luc)
e
0 ng/mL
0,1 ng/mL
0,3 ng/mL
1 ng/mL
3 ng/mL
Reporter
hIL-1β
hTNFα
hIL-6
hIL-6R

Supplementary Figure 4 Related to Figure 4

(**a**) Concentration of human IL-1β and TNFα in peritoneal lavage fluid (left), mouse IL-1β, TNFα and IL-6 in peritoneal lavage fluid (middle) or serum (right) of mice, which were injected i.p. with human IL-1β (300 ng/mouse) or human TNFα (250 ng/mouse) and then sacrificed at different time points.

(**b**) Concentration of mouse IL-1β, TNFα and IL-6 in peritoneal lavage fluid (left) and serum (right) of mice 72 h after CLP procedure.

(**c**) SEAP levels in serum 24 h post implantation and in the peritoneal lavage fluid 48 h post implantation. For detailed information about transfected plasmids and their amounts in each specific experiment, see Supplementary table 1 and 2, respectively. Error bars indicate s.d.

(**d**) The response of the microencapsulated anti-inflammatory device *in vitro* prior to implantation in mice (left) and secretory *Renilla* luciferase (pAS75; SR-Luc) in peritoneal lavage fluid 48 h after microcapsules implantation. SR-Luc was co-transfected along with the anti-inflammatory device but not with the control microcapsules. SR-Luc is comparable among all groups (right).

(**e**) Validation of the chimeric NF-κB-STAT3 sensor. Cells were transfected with the constructs for the anti-inflammatory device, except for the sensor, where pAS60 (TRE-$P_{NF\text{-}\kappa B2}$-P_{MIN}-GV16-myc) was replaced by pAS132 (TRE-$P_{NF\text{-}\kappa B2\text{-}STAT3}$-$P_{MIN}$-GV16-myc). Cells were also transfected with hIL-6 receptor (hIL-6R) where indicated to enable responsiveness to human IL-6. For detailed information about transfected plasmids and their amounts in each specific experiment, see Supplementary table 1 and 2, respectively. Error bars indicate s.d. (n=4).

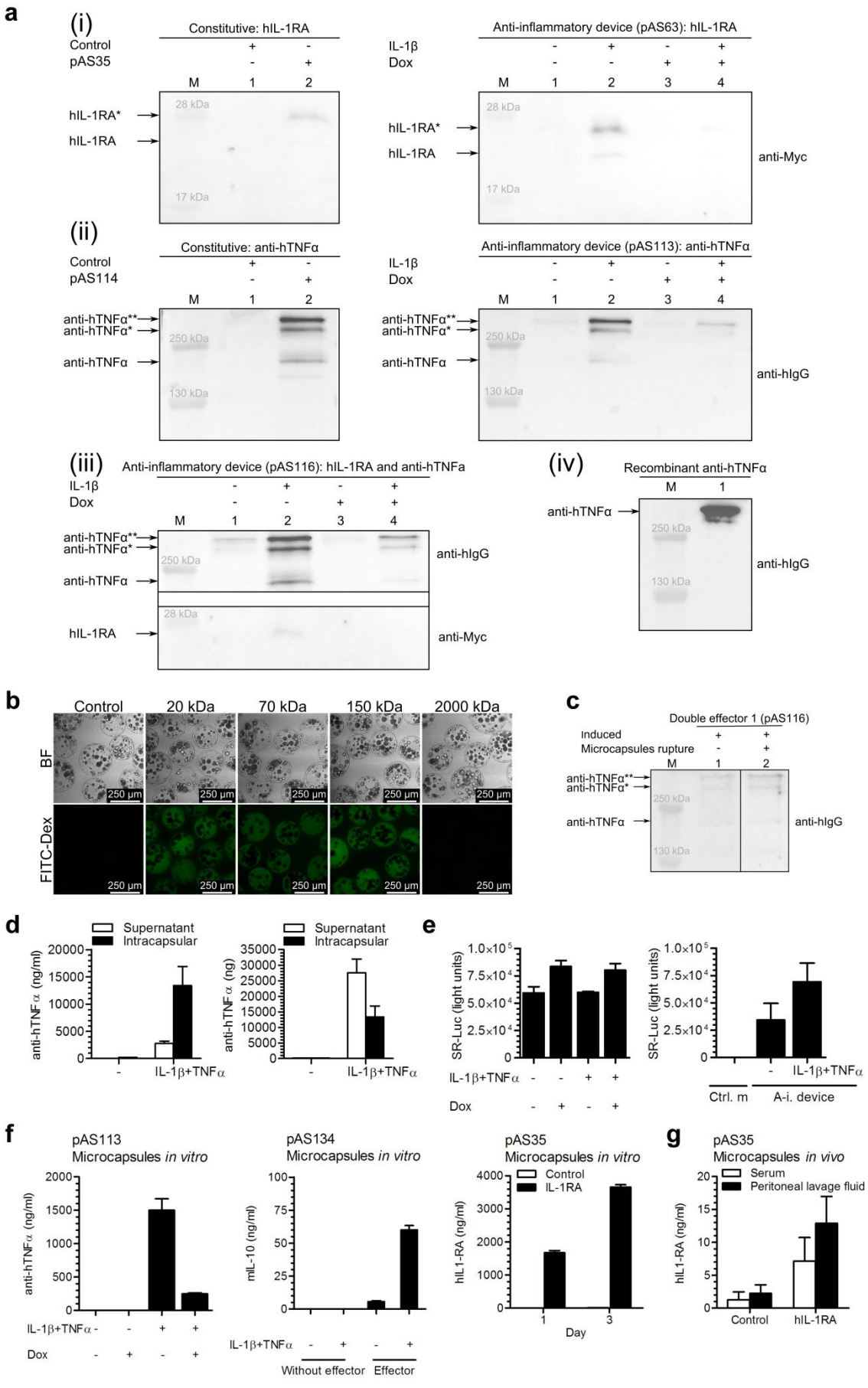
a
(i)
Constitutive: hIL-1RA
Control
pAS35
M 1 2
hIL-1RA*
hIL-1RA
28 kDa
17 kDa
Anti-inflammatory device (pAS63): hIL-1RA
IL-1β
Dox
M 1 2 3 4
anti-Myc
(ii)
Constitutive: anti-hTNFα
Control
pAS114
anti-hTNFα**
anti-hTNFα*
anti-hTNFα
250 kDa
130 kDa
Anti-inflammatory device (pAS113): anti-hTNFα
anti-hIgG
(iii)
Anti-inflammatory device (pAS116): hIL-1RA and anti-hTNFa
(iv)
Recombinant anti-hTNFα
b
Control
20 kDa
70 kDa
150 kDa
2000 kDa
BF
FITC-Dex
250 μm
c
Double effector 1 (pAS116)
Induced
Microcapsules rupture
d
Supernatant
Intracapsular
anti-hTNFα (ng/ml)
anti-hTNFα (ng)
IL-1β+TNFα
e
SR-Luc (light units)
Dox
Ctrl. m
A-i. device
f
pAS113
Microcapsules in vitro
pAS134
Microcapsules in vitro
mIL-10 (ng/ml)
Without effector
Effector
pAS35
Microcapsules in vitro
Control
IL-1RA
hIL1-RA (ng/ml)
Day
g
pAS35
Microcapsules in vivo
Serum
Peritoneal lavage fluid
Control
hIL-1RA

Supplementary Figure 5 Related to Figure 5

(**a**) Western blot analysis of anti-inflammatory effectors from cell culture. (i) Left: Constitutive (pAS35; P_{cmv}-hIL-1RA-myc); and right: inducible (pAS63; TRE-UAS-P_{MIN}-hIL-1RA) production of human interleukin-1 receptor antagonist (hIL-1RA). (ii) Left: Constitutive (pAS114; P_{CMV}-anti-hTNFα Ab); and right: inducible (pAS113; TRE-UAS-P_{MIN}-anti-hTNFα Ab) production of anti-hTNFα antibody (anti-hTNFα). (iii) Anti-inflammatory device-derived (pAS116; TRE-UAS-P_{MIN}-anti-hTNFα Ab-hIL-1RA) production of hIL-1RA and anti-hTNFα. (iv) Recombinant anti-hTNFα used as a control. Amounts of effectors produced from the anti-inflammatory device are comparable to the amounts from a constitutive expression. Putative glycosylation of hIL-1RA is marked as an asterisk. Anti-hTNFα produced in our system has a putative glycosylation at a heavy chain, resulting in tree bands observed (none, only one or both heavy chains glycosylated, marked as an asterisk). Recombinant control, produced from CHO cells however, shows only one substantial band, implicating that biological activity could not be exactly the same. For detailed information about the transfected plasmids and their amounts in each specific experiment, see Supplementary table 1 and 2, respectively.

(**b**) MWCO of the microcapsules. MWCO was determined by FITC-Dextrane (FITC-Dex) of different molecular weights (20 kDa, 70 kDa, 150 kDa, 2000 kDa). Alginate-PLL-alginate microcapsules were incubated overnight at 37 °C with the FITC-Dex solution (20 μg/mL) and then they were washed 3 x using MOPS buffer. Immediately after that, we acquired images using confocal fluorescence microscopy.

(**c**) All forms of anti-hTNFα are able to cross the membrane of microcapsules as observed by western blot analysis, where all bands are present in both, ruptured and unruptured microcapsules. Microcapsules were ruptured by injecting the suspension through 23G needle.

(**d**) Intracapsular amount of anti-hTNFα produced from double effector (pAS116; TRE-UAS-

P_{MIN}-anti-hTNFα Ab-hIL-1RA). Concentration, determined in 10 mL of supernatant or in 1 mL suspension of the same, but previously ruptured microcapsules (left) and total amount of anti-hTNFα (right). For detailed information about transfected plasmids and their amounts in each specific experiment, see Supplementary table 1 and 2, respectively. Error bars indicate s.d. (*n*=3).

(**e**) Secretory *Renilla* luciferase (SR-Luc) control for the *in vitro* (left) and *in vivo* (right) production of anti-inflammatory proteins. SR-Luc was measured either in ruptured microcapsules for *in vitro* assay or in the peritoneal lavage fluid 48 h after microcapsules implantation. SR-Luc is comparable among all groups. For detailed information about transfected plasmids and their amounts in each specific experiment, see Supplementary table 1 and 2, respectively. Error bars indicate s.d. (*n*=4).

(**f**) Production of anti-inflammatory effectors from different constructs and different regimes as indicated in the figure. For detailed information about transfected plasmids and their amounts in each specific experiment, see Supplementary table 1 and 2, respectively. Error bars indicate s.d. (*n*=4).

(**g**) Constitutive *in vivo* production of hIL-RA from the construct pAS35; P_{cmv}-hIL-1RA-myc. For detailed information about transfected plasmid and its amount see Supplementary table 1 and 2, respectively. Error bars indicate s.d. (*n*=4).

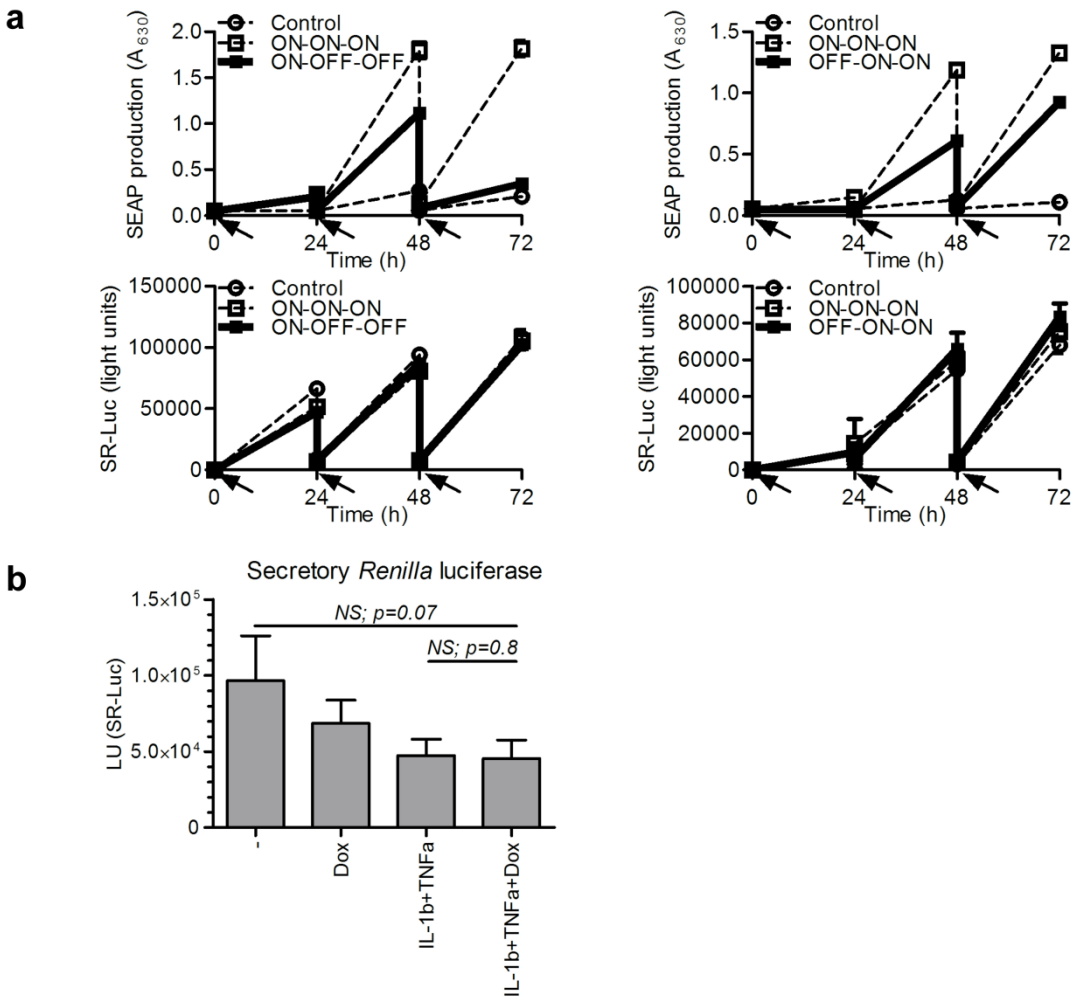
a
SEAP production (A630)
Control
ON-ON-ON
ON-OFF-OFF
OFF-ON-ON
Time (h)
SR-Luc (light units)
b
Secretory Renilla luciferase
LU (SR-Luc)
NS; p=0.07
NS; p=0.8
-
Dox
IL-1b+TNFa
IL-1b+TNFa+Dox
c
Serum anti-hTNFα (ng/mL)
IL-1β+TNFα
IL-1β+TNFα+Dox
p=0.0001
24 h
72 h
120 h
d
Serum mIL-10 (pg/mL)
p=0.03

Supplementary Figure 6 Related to Figure 6

(**a**) The reversibility of the synthetic anti-inflammatory device. Upper left panel: Raw SEAP measurements for *in vitro* shutdown of the system. Anti-inflammatory device-engineered HEK 293T cells (reporter pAS72; TRE-UAS-P_{MIN}-SEAP) were stimulated with interleukin-1β (IL-1β, 1 ng/mL) 6 h after transfection (marked as ON) or left unstimulated (marked as control). 24 h after first stimulation, supernatant containing SEAP was collected and medium was exchanged (indicated by arrows) or in addition, cells were stimulated with IL-1β (1 ng/mL) (marked as ON) or shut down by doxycycline (Dox, 1 μg/mL) (marked as OFF). 48 h and 72 h after first stimulation, procedure was repeated. Upper right panel: Raw SEAP measurements for *in vitro* rebooting of the system shutdown. Anti-inflammatory device-engineered HEK 293T cells (reporter pAS72; TRE-UAS-P_{MIN}-SEAP) were stimulated with IL-1β (1 ng/mL) 6 h after transfection (marked as ON), shut down by Dox (1 μg/mL) (marked as OFF) or left unstimulated (marked as control). 24 h after first stimulation, supernatant containing SEAP was collected and medium was exchanged (indicated by arrows) or in addition, cells were stimulated with IL-1β (1 ng/mL) (marked as ON) or left unstimulated (Control). Lower panel: Secretory *Renilla* luciferase (SR-Luc) used for an internal control. Secretory *Renilla* luciferase is comparable among all groups at any time point in *in vitro* reversibility test.

(**b**) SR-Luc corresponding to the *in vivo* restraint of the full system activation

(**c, d**) Shut down of the anti-inflammatory device *in vivo*. The data represent concentrations corresponding to the results represented in Fig. 6c and 6d. The anti-inflammatory device-engineered HEK 293T cells (effector pAS134; TRE-UAS-P_{MIN}-anti-hTNFα Ab-mIL-10) were microencapsulated, implanted i.p. and fully activated by injection of a combination of 300 ng of hIL-1β and 250 ng of hTNFα per mouse. After 24 h (thin arrow) the device was shut down by an i.v. Dox injection (20 mg/kg). (c) The device was additionally activated and

shut down after 72 h (thick arrow) to reach the relevant time span needed for an observation of the anti-hTNFα antibody kinetics. Serum was collected at different time points and anti-hTNFα antibody or mIL-10 levels were measured.

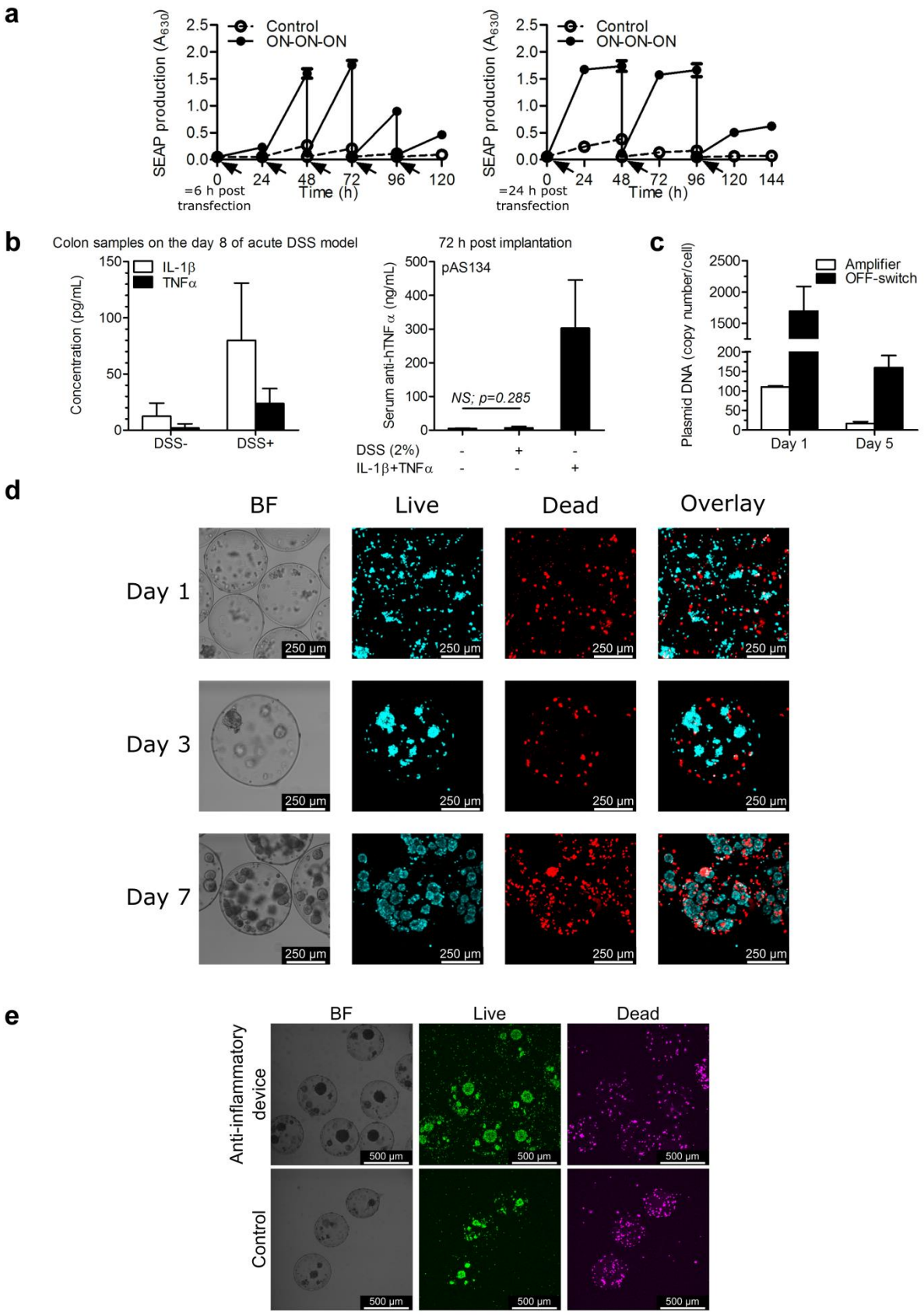
a
SEAP production (A_{630})
Control
ON-ON-ON
Time (h)
=6 h post transfection
=24 h post transfection
b
Colon samples on the day 8 of acute DSS model
IL-1β
TNFα
Concentration (pg/mL)
DSS-
DSS+
72 h post implantation
pAS134
Serum anti-hTNFα (ng/mL)
NS; p=0.285
DSS (2%)
IL-1β+TNFα
c
Amplifier
OFF-switch
Plasmid DNA (copy number/cell)
Day 1
Day 5
d
BF
Live
Dead
Overlay
Day 1
Day 3
Day 7
250 µm
e
BF
Live
Dead
Anti-inflammatory device
Control
500 µm

Supplementary Figure 7 Related to Figure 7

(**a**) A decrease in the system's capacity due to the transient nature of the system. Left: The anti-inflammatory device-engineered HEK 293T cells (reporter pAS72; TRE-UAS-P_{MIN}-SEAP) were stimulated with hIL-1β (1 ng/mL) every 24 h by exchanging the medium (indicated by the arrows). The experiment was started 6 h post transfection, which was represented by 0 h time point. The kinetics of SEAP production was measured every 24 h. Right: The anti-inflammatory device-engineered HEK 293T cells (reporter pAS72; TRE-UAS-P_{MIN}-SEAP) were stimulated with hIL-1β (1 ng/mL) every 48 h by exchanging the medium (indicated by the arrows). The experiment was started 24 h post transfection, which was represented by 0 h time point. The kinetics of SEAP production was measured every 24 h to observe a cumulative SEAP production. Error bars indicate s.d. (*n*=4).

(**b**) DSS-induced colitis increased endogenous inflammatory cytokines in the supernatants of colon biopsy samples but does not activate the device. Left: Concentration of endogenous mIL-1β and mTNFα in the supernatants of colon biopsy samples on the 8^{th} day of DSS-induced acute colitis (*n*=6 biopsy samples per mouse, 2 mice per group) Right: The activation of the implanted anti-inflammatory device by DSS. The mice were given either water or 2 % DSS for 8 days and on the 5^{th} day of this time-course experimental model, the microcapsules containing anti-inflammatory device-engineered cells (effector construct pAS134; TRE-UAS-P_{MIN}-anti-hTNFα Ab-mIL-10, Supplementary Table 1) were implanted i.p. Positive control group was stimulated with a combination of 300 ng of hIL-1β and 250 ng of hTNFα per mouse 1 h post implantation. Concentration of anti-hTNFα was measured 72 h post implantation (on the 8^{th} day of the experimental colitis model) (*n*=3).

(**c**) A decrease in the system's capacity due to the transient nature of the system. HEK 293T cells were transfected according to the Supplementary Table 2 and lysed after 1 or 5 days. Samples were analyzed by real-time quantitative PCR using the primers to specifically

amplify the amplifier or the inducible OFF-switch constructs. The plasmid copy number in the samples was estimated from the standard curves of the known amounts of the respective constructs spiked into the lysate and recalculated per cell (n = 2 biological replicates tested at 2 different dilutions of the respective lysate).

(**d**) Confocal fluorescence microscopy of the microcapsules in the *in vitro* culture as observed 1, 3 or 7 days after microencapsulation procedure. A large majority of the microencapsulated cells remained viable and divided as observed by aggregates formed. Live and dead cells were stained with Hoechst and propidium iodide, respectively.

(**e**) Confocal fluorescence microscopy of the microcapsules after having been implanted in peritoneal cavity of mice for 3 days. Cells remain viable during the course of the experiments, conducted in this study. Live and dead cells were stained with Hoechst and propidium iodide, respectively.

EXTENDED EXPERIMENTAL PROCEDURES

The ability of antibody molecules to transverse the alginate-PLL-alginate membrane

Anti-hTNFα antibody is a glycosylated, 150 kDa molecule and since the ability of antibody molecules to transverse the alginate-PLL-alginate membrane is somewhat controversial[1,2], we investigated whether the anti-hTNFα is able to cross the membrane of microcapsules in our system. First, we have shown that 20 kDa, 70 kDa and also 150 kDa, but not 2000 kDa FITC-Dextrane molecules are able to cross the membrane (Supplementary Fig. 5b). Next, we have shown that glycosylated, higher molecular mass forms of the antibody are secreted from the microcapsules, since we detected corresponding bands in the western blot analysis of either intact or ruptured microcapsules (Supplementary Fig. 5c). The intracapsular concentration of anti-hTNFα was somewhat higher than the concentration in the supernatant, nevertheless, the majority of anti-hTNFα was released into the supernatant (Supplementary Fig. 5d).

Confocal fluorescence microscopy related to Supplementary Fig. 3b, 3c, 5b and 7

For the *in vitro* direct observation of the system's performance, HEK 293T cells were seeded onto 8-well microscopic chambers (Ibidi) at a density of 5 x 10^4 cells per well. Cells were transfected with the constructs pAS97 (observation of the sensor activity) and/or pAS98 (observation of the amplifier activity), pAS72, pAS67, pAS58, pAS75 and pmCherry-C1 (detailed description in the Supplementary Table 1). 4 h after transfection, doxycycline (1 μg/mL) was added to the samples, which we wanted to shut down. 24 h after transfection, the system was stimulated with human IL-1β (R&D Systems, Inc., Minneapolis, USA) at a final concentration of 1 ng/mL. 4 h after stimulation, medium was removed and cells were washed 3 x using fresh medium to remove an input signal. After 24 h, the responsiveness of the system was visualized and microscopic images were acquired using the Leica TCS SP5 inverted laser-scanning microscope on a Leica DMI 6000 CS module equipped with a HCX PL Fluotar L 20 x, numerical aperture 0.4 (Leica Microsystems, Wetzlar, Germany). A 514-

nm laser line of a 100-mW argon laser with 25 % laser power was used for mCitrine excitation, and the emitted light was detected between 520 and 580 nm. A 50-mW 405-nm diode laser was used for tagBFP excitation and the emitted light was detected between 420 and 460 nm. A 1-mW 543-nm HeNe laser was used for mCherry excitation and the emitted light was detected between 560 and 630 nm. Leica LAS AF software was used for acquisition and ImageJ software was used for image processing.

To determine an approximate MWCO of the microcapsules, we observed the permeability of microcapsules for fluorescein isothiocyanate-dextran (FITC-Dex, Sigma Aldrich) of different molecular weights (20 kDa, 70 kDa, 150 kDa and 2000 kDa). Alginate-PLL-alginate microcapsules were incubated overnight at 37 °C with the FITC-Dex solution (20 μg/mL) and then they were washed 3 x using MOPS buffer. Immediately after that, we acquired images using confocal fluorescence microscopy. A 488 Argon laser was used for FITC-Dex excitation and the emitted light was detected between 502 and 553 nm.

To observe integrity of microcapsules and viability of cells after 3 day *in vivo* experiment we made peritoneal lavage and collected microcapsules. We stained microcapsules with Hoechst at a final concentration of 1 μg/mL (ImmunoChemistry Technologies, LLC, 639) for live cells and propidum iodide at a final concentration of 0.6 μg/mL (Sigma Aldrich, P4864) for dead cells. After 30 min incubation at 37 °C, images were acquired. A 1-mW 543-nm HeNe laser was used for propidium iodide excitation and the emitted light was detected between 600 and 670 nm. A 405 Diode laser was used for Hoechst excitation and the emitted light was detected between 429 and 509 nm. The same procedure was followed for the visualization of the microencapsulated cells after 1, 3 and 7 days in the *in vitro* culture.

Cytokine detection related to Supplementary Fig. 4a, 4b and 7b

Serum and peritoneal lavage fluid of mice were collected as described in the Materials and Methods section (Animal Models) in the main article. Colon biopsy samples were prepared by following the described[3] "Full-thickness organ culture" method to determine a concentration of inflammatory cytokines in the supernatants. Inflammatory cytokine levels were measured by a sandwich ELISA according to the manufacturer's instructions (eBioscience) as follows: human IL-1β was detected by human IL-1 beta ELISA Ready-SET-Go! (eBioscience, 88-7010), human TNF-α by human TNF alpha ELISA Ready-SET-Go! (eBioscience, 88-7346), mouse IL-1β by mouse IL-1 beta ELISA Ready-SET-Go! (eBioscience, 88-7013), mouse TNFα by mouse TNF alpha ELISA Ready-SET-Go! (eBioscience, 88-7324), mouse IL-6 by mouse IL-6 ELISA Ready-SET-Go! (eBioscience, 88-7064).

Western blotting related to Supplementary Fig. 5a and 5c

Supernatants from pAS35 (CMV promoter-driven hIL-1RA-myc production), pAS113 (NF-κB-driven anti-hTNFα antibody expression), pAS114 (CMV promoter-driven anti-hTNFα antibody) and pAS116 (NF-κB-driven anti-hTNFα antibody-hIL-1RA-myc double effector expression unit) (detailed description in the Supplementary Table 1) were analyzed for hIL-RA-myc and anti-hTNFα antibody expression. 30 μL of a cell culture supernatant, expressing certain protein was mixed with 4xSDS buffer without reducing agent, boiled for 5 min at 95 °C and centrifuged at 14000g for 3 min. Proteins were resolved on 12 % SDS-PAGE and analyzed by a standard western blotting procedure. hIL-1RA-myc was detected by rabbit anti-myc IgG primary antibody (1: 500) (Sigma Aldrich, C3956) and goat polyclonal to rabbit IgG (HRP) secondary antibody (1: 3000) (Abcam, ab6721), while anti-hTNFα antibody was detected by rabbit polyclonal secondary antibody to human IgG – H and L (HRP) (1: 3000) (Abcam, ab 6759). Recombinant anti-hTNF-α-hIgG1 (InvivoGen, htnfa-mab1) and an empty vector pcDNA3.1 were used as controls.

Estimation of the plasmid copy number per cell related to Supplementary Fig. 7c

A decrease in the system's capacity due to the transient nature of the transfection was estimated by real-time quantitative PCR analysis. HEK 293T cells were seeded in 10 cm tissue culture petri dish (TPP), transfected at 50-70 % confluency according to the Supplementary Table 2, washed with PBS twice, trypsinized and collected by centrifugation (1400 rpm, 8 min) 1 or 5 days post transfection. The number of cells was determined by Trypan blue staining. Cell lysis was performed by resuspending the pellet in 500 μL MQ, incubation at 4 °C for 12 h, freezing at -70 °C, boiling at 95 °C for 10 min and centrifugation (12000 rpm, 20 min). Supernatants were transferred to fresh tubes and stored for analysis at -20 °C. Samples were diluted 1000-fold or 10000-fold and analyzed by real-time quantitative PCR using the primers to specifically amplify the plasmid encoding the amplifier (F: 5'-ACTGTCCTCCGAGAGATCTTAGAGGG-3' R: 5'-GCGACACTCCCAGTTGTTCTTCAG-3') or the inducible OFF-switch (F: 5'-GGCGGTGGTGCTTTGTCTCC-3' R: 5'-CTCCAGCATCACATTTCTGTACACG-3') constructs. Real-time PCR was performed using Power SYBR Green PCR Master Mix (Roche) in a Roche LightCycler® 480. Known amounts of the corresponding plasmids were spiked into the 1000-fold or 10000-fold diluted lysate of the non-transfected cells (prepared as described above) to obtain the standard curves (C_t plotted against log plasmid copy number) under the same cycling conditions. The plasmid copy number in the samples was estimated from the standard curves and recalculated per cell.

Supplementary Table 1. Genetic constructs used and designed in this study

Name of the plasmid	Description of gene construct	Reference
pISRE-Luc	Mammalian expression vector encoding P_{ISRE}-P_{TAL}-driven luciferase expression unit (P_{ISRE}-P_{TAL}-Lucuferase-pA). pISRE-Luc contains five copies of the ISRE-binding sequence, located upstream of the TATA-like promoter (P_{TAL}) region from the herpes simplex virus thymidine kinase (HSV-TK) promoter.	Clontech
pcDNA3.1	Mammalian expression vector (P_{CMV}-MCS-pA)	Life Technologies
pFLAG-CMV3	Mammalian expression vector for secretory proteins (P_{CMV}-preprotrypsin leader sequence-flag-tag-MCS-pA)	Sigma Aldrich
pMF208	Mammalian expression vector encoding SV40-PIR3-driven SEAP expression (P_{PIR}ON-SEAP- pA)[4]	Kindly provided by Professor Dr. Martin Fussenegger (Institute of Biotechnology, Swiss Federal Institute of Technology, ETH Zürich)[4]
phRL-TK	Mammalian expression vector for constitutive HSV-TK-promoter-driven renilla luciferase expression (phRL-TK-rLuc)	Promega
pSGVP	Mammalian expression vector for constitutive SV40 promoter-driven GV16 expression (GV16 is Gal4-VP16 transcriptional activator).	Kindly provided by Professor Dr Mark Ptashne (Memorial Sloan Kettering Cancer Center, New York, NY,

		USA)[5]
pLVPT-rtTR-KRAB-2SM2	Lentiviral vector containing rtTR-NLS-KRAB (reverse tetracycline repressor fused to nuclear localization signal and KRAB transcription repression domain)	(plasmid 11652, Addgene)[6]
pMF111	Mammalian expression vector pTBC1 encoding tetracycline-responsive element TetO7-driven SEAP expression.	Kindly provided by Professor Dr. Martin Fussenegger (Institute of Biotechnology, Swiss Federal Institute of Technology, ETH Zürich)[7]
pmCherry-C1	Mammalian expression vector encoding constitutive CMV promoter-driven expression of pmCherry-C1 (Clontech). Plasmid ensures constitutive expression of mCherry, and was used to normalize levels of transfection in confocal microscopy experiments.	Clontech
pORF9-hIL06Ra	Mammalian expression vector for constitutive hEF1/HTLV promoter-driven human IL6R (IL-6 receptor, isoform 1) expression.	InvivoGen
pAS34	Mammalian expression vector encoding constitutive HSV-TK promoter-driven hIL-1RA-myc expression unit (P_{HSV-TK}-hIL-1RA-myc). hIL-1RA was PCR amplified from pORF9-hIL1RNa (InvivoGen, commercially available vector) (5'-caggaagcttggcattccggtactgttggtaaagccaccATGGAAATCTGCAGAGGCCTCCGC-3', 5'-ggcctctagaattacagatcctcttcagagatgagtttctgctcCTCGTCCTCCTGGAAGTAGAATTTGGTGACC-3') adding C-terminal myc-tag and cloned into the corresponding sites (HindIII/XbaI) of phRL-TK, replacing chimeric intron-renilla luciferase cassette.	This work
pAS35	Mammalian expression vector encoding constitutive CMV promoter-driven hIL-1RA-myc expression unit (P_{cmv}-hIL-1RA-myc). hIL-1RA was PCR amplified from pORF9-hIL1RNa (InvivoGen, commercially available vector) (5'-caggaagcttCGACCCTCTGGGAGAAAATCCAGC-3', 5'-ggcctctagaattacagatcctcttcagagatgagtttctgctcCTCGTCCTCCTGGAAGTAGAATTTGGTG	This work

	ACC-3') omitting signal sequence but adding C-terminal myc-tag and cloned into the corresponding sites (HindIII/XbaI) of pFLAG-CMV3, creating secretory of hIL-1RA (preprotrypsin leader sequence).	
pAS36	Mammalian expression vector encoding $P_{NF\text{-}\kappa B1}$-P_{TAL}-driven luciferase expression unit ($P_{NF\text{-}\kappa B1}$-P_{TAL}-Luc). The NF-κB responsive element (sequence: GGGAATTTCCGGGAATTTCCGGGAATTTCCGGGAATTTCC) was cloned into the corresponding sites (NheI/BglII) of the pISRE-Luc vector, replacing the P_{ISRE}.	This work
pAS37	Mammalian expression vector encoding $P_{NF\text{-}\kappa B2}$-P_{TAL}-driven luciferase expression unit ($P_{NF\text{-}\kappa B2}$-P_{TAL}-Luc). The NF-κB responsive element (sequence: GGGAATTTCCGGGGACTTTCCGGGAATTTCCGGGGACTTTCCGGGAATTTCC) was cloned into the corresponding sites (NheI/BglII) of the pISRE-Luc vector, replacing the P_{ISRE}.	This work
pAS40	Mammalian expression vector encoding $P_{NF\text{-}\kappa B2}$-P_{MIN}-driven luciferase expression unit ($P_{NF\text{-}\kappa B2}$-P_{MIN}-Luc). We excised P_{TAL} from pAS37 with BglII/HindIII and replaced it with P_{MIN} minimal promoter (sequence: TAGAGGGTATATAATGGAAGCTCGACTTCCAG).	This work
pAS44	Mammalian expression vector encoding $P_{NF\text{-}\kappa B2}$-P_{MIN}-driven GV16-myc expression unit (GV16-myc, Gal4-VP16 transcriptional activator with C-terminal myc-tag,) ($P_{NF\text{-}\kappa B2}$-P_{MIN}-GV16-myc). GV16 was PCR amplified from pSGVP vector adding C-terminal myc-tag with the reverse primer (5'-cagg<u>aagcttg</u>gcattccggtactgttggtaaagccaccATGAAGCTACTGTCTTCTATCGAACAAGC-3' and 5'-ggcc<u>tctaga</u>attacagatcctcttcagagatgagtttctgctcCCCACCGTACTCGTCAATTCCAAGGGC-3') and cloned into the corresponding sites (HindIII/XbaI) of pAS40, replacing the luciferase expression unit.	This work
pAS48	Mammalian expression vector encoding $P_{NF\text{-}\kappa B2}$-P_{MIN}-driven GV16 expression unit (GV16, Gal4-VP16 transcriptional activator) ($P_{NF\text{-}\kappa B2}$-P_{MIN}-GV16). GV16 was PCR amplified from pSGVP vector (5'-cagg<u>aagcttg</u>gcattccggtactgttggtaaagccaccATGAAGCTACTGTCTTCTATCGAACAAGC-3' and 5'-ggcc<u>tctaga</u>aTTACCCACCGTACTCGTCAATTCCAAGGGC-3') and cloned into the corresponding sites (HindIII/XbaI) of pAS40, replacing the luciferase expression	This work

	unit.	
pAS49	Mammalian expression vector encoding UAS-P_{MIN}-driven luciferase expression unit. Luciferase is expressed only in the presence of GV16, which binds to UAS sequence (5 consecutive Gal4 binding sites), placed directly upstream P_{MIN} (UAS-P_{MIN}-Luc, UAS, upstream activatory sequence). UAS (sequence: CGGAGTACTGTCCTCCGAGCGGAGTACTGTCCTCCGAGCGGAGTACTGTCCTC CGAGCGGAGTACTGTCCTCCGAGCGGAGTACTGTCCTCCGAG) was cloned into the corresponding sites (NheI/BglII) of pAS40, replacing the $P_{NF\text{-}\kappa B2}$.	This work
pAS51	Mammalian expression vector encoding TRE-UAS-P_{MIN}-driven luciferase expression unit (TRE-UAS-P_{MIN}-Luc). Luciferase could be repressed by rtTR-NLS-KRAB-2SM2 which binds to 7 consecutive Tet-binding sites (Tet-responsive element; TRE) placed directly upstream UAS in the presence of doxycycline. TRE was PCR-amplified from pMF111 (5'-ggccggtaccCTCGAGTTTACCACTCCC-3', 5'-ggccgctagcGAGCTCGACTTTCACTTTTCTC-3') and cloned into the corresponding sites (KpnI/NheI) directly upstream UAS of pAS49.	This work
pAS53	Mammalian expression vector encoding UAS-P_{MIN}-driven GV16 expression unit (UAS-P_{MIN}-GV16). The construct is based on a positive feedback loop of an orthogonal transcriptional activator GV16, which amplifies its own transcription by binding UAS placed directly upstream P_{MIN}. GV16 was PCR amplified from pSGVP vector (5'-caggaagcttggcattccggtactgttggtaaagccaccATGAAGCTACTGTCTTCTATCGAACAAGC-3' and 5'-ggcctctagaaTTACCCACCGTACTCGTCAATTCCAAGGGC-3') and cloned into the corresponding sites (HindIII/XbaI) of pAS49, replacing the luciferase expression unit.	This work
pAS54	Mammalian expression vector encoding UAS-P_{MIN}-driven GV16-myc expression unit (UAS-P_{MIN}-GV16-myc). The construct is based on a positive feedback loop of an orthogonal transcriptional activator GV16, which amplifies its own transcription by binding UAS placed directly upstream P_{MIN}. GV16 was PCR amplified from pSGVP vector adding C-terminal myc-tag with the reverse primer (5'-caggaagcttggcattccggtactgttggtaaagccaccATGAAGCTACTGTCTTCTATCGAACAAGC-3' and 5'-ggcctctagaattacagatcctcttcagagatgagtttctgctcCCCACCGTACTCGTCAATTCCAAGGGC-3') and cloned into the corresponding sites (HindIII/XbaI) of pAS49, replacing the luciferase expression unit.	This work

pAS58	The inducible off-switch construct. Mammalian expression vector encoding constitutive CMV-promoter-driven rtTR-NLS-KRAB expression (P_{CMV}-rtTR-NLS-KRAB). rtTR-NLS-KRAB binds 7 consecutive Tet-binding sites (Tet-responsive element; TRE) and silences gene expression several kilobases upstream and downstream only in the presence of a doxycycline. rtTR-NLS-KRAB-2SM2 was PCR-amplified from pLVPT-rtTR-KRAB-2SM2 (5'-ggccggtaccGCCACCATGGCTAGACTGGACAAGAGCAAAGTCATAAACGGC-3', 5'-ccgggaattcTTAAACTGATGATTTGATTTCAAATGCAGTCTCTGAATCAGG-3') and cloned into the corresponding sites (KpnI/EcoRI) of pcDNA3.1.	This work
pAS60	The sensor construct. Mammalian expression vector encoding TRE-$P_{NF-κB2}$-P_{MIN}-driven GV16-myc expression unit (TRE-$P_{NF-κB2}$-P_{MIN}-GV16-myc). TRE was PCR-amplified from pMF111 (5'-ggccggtaccCTCGAGTTTACCACTCCC-3', 5'-ggccgctagcGAGCTCGACTTTCACTTTTCTC-3') and cloned into the corresponding sites (KpnI/NheI) directly upstream UAS of pAS44.	This work
pAS62	The amplifier construct. Mammalian expression vector encoding TRE-UAS-P_{MIN}-driven GV16-myc expression unit (TRE-UAS-P_{MIN}-GV16-myc). TRE was PCR-amplified from pMF111 (5'-ggccggtaccCTCGAGTTTACCACTCCC-3', 5'-ggccgctagcGAGCTCGACTTTCACTTTTCTC-3') and cloned into the corresponding sites (KpnI/NheI) directly upstream UAS of pAS54.	This work
pAS63	Mammalian expression vector encoding TRE-UAS-P_{MIN}-driven human IL-1RA expression unit (TRE-UAS-P_{MIN}-hIL-1RA). hIL-1RA was excised from pAS34 using HindIII/XbaI and cloned into the corresponding sites of pAS51 vector, replacing luciferase cassette.	This work
pAS67	The positive feedback "thresholder" construct. Mammalian expression vector encoding constitutive HSV-TK promoter-driven Gal4-myc expression unit (P_{HSV-TK}-G-myc). Gal4 was PCR amplified from pSGVP adding C-terminal myc-tag with the reverse primer (5'-caggaagcttggcattccggtactgttggtaaagccaccATGAAGCTACTGTCTTCTATCGAACAAGC-3', 5'-ggcctctagaattacagatcctcttcagagatgagtttctgctcCGATACAGTCAACTGTCTTTGACC-3') and cloned into the corresponding sites (HindIII/XbaI) of phRL-TK, replacing chimeric intron-renilla luciferase cassette.	This work
pAS72	Mammalian expression vector encoding TRE-UAS-P_{MIN}-driven secretory alkaline phosphatase (SEAP) expression unit (TRE-UAS-P_{MIN}-SEAP). SEAP was PCR-amplified from pMF208[4] vector (5'-	This work

	gtctaagcttggcattccggtactgttggtaaagccaccATGCTGCTGCTGCTGCTGCTGCTGGGCC-3', 5'-ggccactagtttatcaTGTCTGCTCGAAGCGGCCGGCC-3'), digested with HindIII/SpeI and cloned into the HindIII/XbaI digested pAS62, thereby giving SpeI/XbaI mixed site at 3', replacing GV16-myc.	
pAS75	Mammalian expression vector encoding CMV-driven secretory renilla luciferase (SR-Luc) expression unit (P_{CMV}-SR-Luc). Renilla luciferase was PCR-amplified from phRL-TK (5'-ggccaagcttGCTTCCAAGGTGTACGACCCCG-3', 5'-ccggtctagaaTTACTGCTCGTTCTTCAGC-3') and cloned into the corresponding sites (HindIII/XbaI) of pFLAG-CMV3, creating secretory form of renilla luciferase (preprotrypsin leader sequence).	This work
pAS97	Mammalian expression vector encoding TRE-$P_{NF\text{-}\kappa B2}$-P_{MIN}-driven GV16-myc-2A-mCitrine expression unit (TRE-$P_{NF\text{-}\kappa B2}$-P_{MIN}-GV16-myc-2A-mCit). 2A-mCit was PCR-amplified (5'-CATCTCTGAAGAGGATCTGggcgccggaagcggaGAGGGGAGAGGAAGTCTTCTGACC-3', 5'-CGGCCGGCCGCCCCGACTCTAGAATTAgcgcgcCTTGTACAGCTCGTCCATGCCG-3') from 10x[b]_l4_[CMV]_l2_TALA:KRAB:t2A:mCit[8] and pAS60 was PCR amplified (5'-CGGCATGGACGAGCTGTACAAGgcgcgcTAATTCTAGAGTCGGGGCGGCC-3', 5'-CCTCTCCCCTCtccgcttccggcgccCAGATCCTCTTCAGAGATGAGTTTCTGCTCC-3'). Both fragments were assembled using Gibson assembly method[9], introducing 2A-mCit cassette into the sensor construct downstream of GV16-myc. 2A amino acid sequence: GSGEGRGSLLTCGDVEENPGP[10].	This work
pAS98	Mammalian expression vector encoding TRE-UAS-P_{MIN}-driven GV16-myc-2A-tagBFP expression unit (TRE-UAS-P_{MIN}-GV16-myc-2A-tagBFP). First, 2A-TagBFP was PCR amplified (5'-atcgggcgccggaagcggaGAGGGGAGAGGAAGTCTTCTGACCTGCGG-3', 5'-cgatgcgcgcATTGAGCTTGTGCCCCAGTTTGCTAGGGAGG-3') from 10x[a]_l4_[CMV]_l2_TALB:KRAB:t2A:BFP[8] and ligated into the corresponding sites (KasI/BssHII) of pAS97. Then this construct was digested with EcoRI/XbaI and ligated into the corresponding sites of pAS62, introducing 2A-tagBFP cassette into the amplifier construct downstream of GV16-myc. 2A amino acid sequence: GSGEGRGSLLTCGDVEENPGP[10].	This work
pAS108	Mammalian expression vector for constitutive CMV promoter-driven luciferase expression	This work

	(P_{CMV}-Luc). CMV promoter was excised from pcDNA3.1 using BglII/HindIII and cloned into the corresponding sites of pAS51 vector, replacing P_{MIN}.	
pAS109	Mammalian expression vector for constitutive CMV promoter-driven SEAP expression (P_{CMV}-SEAP). CMV promoter was excised from pcDNA3.1 using BglII/HindIII and cloned into the corresponding sites of pAS72 vector, replacing P_{MIN}.	This work
pAS113	Mammalian expression vector encoding TRE-UAS-P_{MIN}-driven anti-hTNFα antibody expression unit (TRE-UAS-P_{MIN}-anti-hTNFα Ab). Anti-hTNFα antibody was excised from pAS117 using HindIII/XbaI and cloned into the corresponding sites of pAS51 vector, replacing luciferase cassette.	This work
pAS114	Mammalian expression vector encoding constitutive CMV promoter-driven anti-hTNFα antibody (P_{CMV}-anti-hTNFα Ab). Anti-hTNFα antibody was excised from pAS117 using HindIII/XbaI and cloned into the corresponding sites of pcDNA3.1 vector.	This work
pAS115	Mammalian expression vector encoding TRE-UAS-P_{MIN}-driven anti-hTNFα antibody-2A-tagBFP expression unit (TRE-UAS-P_{MIN}-GV16-myc-2A-anti-hTNFα Ab). Anti-hTNFα antibody was excised from pAS117 using HindIII/KasI and cloned into the corresponding sites of pAS98 vector, replacing GV16-myc cassette.	This work
pAS116	Mammalian expression vector encoding TRE-UAS-P_{MIN}-driven anti-hTNFα antibody-hIL-1RA-myc double effector expression unit (TRE-UAS-P_{MIN}-anti-hTNFα Ab-hIL-1RA; DE1). hIL-1RA was PCR amplified from pORF9-hIL1RNa (InvivoGen, commercially available vector) (5'-gtctggcgccggaagcggagaggggagaggaagtcttctgacctgcggagacgtcgaagagaatcctggacccATGGAAATCTGCAGAGGCCTCC-3', 5'-ggcctctagaattacagatcctcttcagagatgagtttctgctcCTCGTCCTCCTGGAAGTAGAATTTGGTGACC-3') adding N-terminal 2A peptide and C-terminal myc-tag and cloned into the corresponding sites of pAS115, replacing 2A-tagBFP (KasI/XbaI). Amino acid sequence with annotation: MGVKVLFALICIAVAEAEVQLVESGGGLVQPGRSLRLSCAASGFTFDDYAMHWVRQAPGKGLEWVSAITWNSGHIDYADSVEGRFTISRDNAKNSLYLQMNSLRAEDTAVYYCAKVSYLSTASSLDYWGQGTLVTVSSASTKGPSVFPLAPSSKSTSGGTAALGCLVKDYFPEPVTVSWNSGALTSGVHTFPAVLQSSGLYSLSSVVTVPSSSLGTQTYICNVNHKPSNTKVDKKVEPKSCDKTHTCPPCPAPELLGGPSVFLFPPKPKDTLMISRTPEVTCVVVDVSHEDPEVKFNWYVDGVEVHNAKTKPREEQYNSTYRVVSVLTVL	

	HQDWLNGKEYKCKVSNKALPAPIEKTISKAKGQPREPQVYTLPPSRDELTKNQVS LTCLVKGFYPSDIAVEWESNGQPENNYKTTPPVLDSDGSFFLYSKLTVDKSRWQQ GNVFSCSVMHEALHNHYTQKSLSLSPGKRAKRGSGEGRGSLLTCGDVEENPGPM GVKVLFALICIAVAEADIQMTQSPSSLSASVGDRVTITCRASQGIRNYLAWYQQKP GKAPKLLIYAASTLQSGVPSRFSGSGSGTDFTLTISSLQPEDVATYYCQRYNRAPYT FGQGTKVEIKTVAAPSVFIFPPSDEQLKSGTASVVCLLNNFYPREAKVQWKVDNA LQSGNSQESVTEQDSKDSTYSLSSTLTLSKADYEKHKVYACEVTHQGLSSPVTKSF NRGECRAKRGAGSGEGRGSLLTCGDVEENPGPMEICRGLRSHLITLLLFLFHSETIC RPSGRKSSKMQAFRIWDVNQKTFYLRNNQLVAGYLQGPNVNLEEKIDVVPIEPHA LFLGIHGGKMCLSCVKSGDETRLQLEAVNITDLSENRKQDKRFAFIRSDSGPTTSFE SAACPGWFLCTAMEADQPVSLTNMPDEGVMVTKFYFQEDEEQKLISEEDL Gaussia luciferase signal peptide[11] anti-hTNFα Ab heavy chain variable region[12] RAKR motif for cleavage by furine hIg gamma-1 chain constant region 2A peptide anti-hTNFα Ab light chain variable region[12] Ig kappa chain constant region hIL-1RA-myc tag	
pAS117	Synthetic gen, encoding anti-hTNFα antibody Adalimumab[12], (anti-hTNFα Ab). Nucleotide sequence: aagcttggcattccggtactgttggtaaagccaccATGGGCGTGAAGGTGCTGTTCGCCCTGATCTG TATCGCCGTGGCCGAGGCCGAAGTGCAGCTGGTGGAATCTGGCGGAGGACTG GTGCAGCCTGGCAGAAGCCTGAGACTGAGCTGTGCCGCCAGCGGCTTCACCTT CGACGACTACGCCATGCACTGGGTGCGCCAGGCCCCTGGAAAAGGCCTGGAAT GGGTGTCCGCCATCACCTGGAACAGCGGCCACATCGATTACGCCGACAGCGTG GAAGGCCGGTTCACCATCAGCCGGGACAACGCCAAGAACAGCCTGTACCTGC AGATGAACTCCCTGCGGGCCGAGGACACCGCCGTGTACTACTGTGCCAAGGTG TCCTACCTGAGCACCGCCAGCAGCCTGGATTATTGGGGCCAGGGCACACTCGT GACCGTGTCTAGCGCCAGCACAAAGGGCCCCAGCGTGTTCCCTCTGGCCCCTA GCAGCAAGAGCACAAGCGGAGGAACAGCCGCCCTGGGCTGCCTCGTGAAGGA CTACTTTCCCGAGCCCGTGACAGTGTCCTGGAATAGCGGAGCCCTGACCAGCG	This work

GCGTGCACACCTTTCCAGCTGTGCTGCAGAGCAGCGGCCTGTACAGCCTGAGC

AGCGTCGTGACTGTGCCCAGCAGCTCTCTGGGCACCCAGACCTACATCTGCAA

CGTGAACCACAAGCCCAGCAACACCAAGGTGGACAAGAAGGTGGAACCCAAG

AGCTGCGACAAGACCCACACCTGTCCCCCTTGTCCTGCCCCCGAACTGCTGGG

AGGCCCTTCCGTGTTCCTGTTCCCCCCAAAGCCCAAGGACACCCTGATGATCA

GCCGGACCCCCGAAGTGACCTGCGTGGTGGTGGATGTGTCCCACGAGGACCCT

GAAGTGAAGTTTAATTGGTACGTGGACGGCGTGGAAGTGCACAATGCCAAGA

CCAAGCCTAGAGAGGAACAGTACAACTCCACCTACCGGGTGGTGTCCGTGCTG

ACCGTGCTGCATCAGGACTGGCTGAACGGCAAAGAGTACAAGTGCAAAGTGT

CCAACAAGGCCCTGCCTGCCCCCATCGAGAAAACCATCAGCAAGGCCAAGGG

CCAGCCCCGCGAACCCCAGGTGTACACACTGCCCCCAAGCAGGGACGAGCTG

ACCAAGAACCAGGTGTCCCTGACCTGTCTCGTGAAAGGCTTCTACCCCAGCGA

CATTGCCGTGGAATGGGAGAGCAACGGCCAGCCCGAGAACAACTACAAGACC

ACCCCCCCTGTGCTGGACAGCGACGGCTCATTCTTCCTGTACTCCAAGCTGACA

GTGGACAAGTCCCGGTGGCAGCAGGGCAACGTGTTCAGCTGCAGCGTGATGCA

CGAGGCCCTGCACAACCACTACACCCAGAAGTCCCTGAGCCTGAGCCCCGGCA

AGAGAGCCAAGAGAGGATCTGGCGAGGGCAGAGGCAGCCTGCTGACATGTGG

CGACGTGGAAGAGAACCCAGGCCCTATGGGAGTGAAAGTGCTGTTTGCTCTGA

TCTGCATTGCTGTGGCTGAAGCCGACATCCAGATGACCCAGAGCCCCTCTAGC

CTGAGCGCCAGCGTGGGCGACAGAGTGACCATCACATGCAGAGCCAGCCAGG

GCATCCGGAACTACCTGGCCTGGTATCAGCAGAAGCCCGGCAAGGCCCCTAAG

CTGCTGATCTACGCCGCCTCCACACTGCAGAGCGGAGTGCCCTCCAGATTTTCC

GGCAGCGGCTCCGGCACCGACTTCACCCTGACAATCAGCTCCCTGCAGCCAGA

GGACGTGGCCACCTACTACTGCCAGCGGTACAACAGAGCCCCCTACACCTTCG

GACAGGGCACAAAGGTGGAAATCAAGACCGTGGCCGCTCCCTCCGTGTTCATC

TTCCCACCTAGCGACGAGCAGCTGAAGTCCGGCACAGCCTCTGTCGTGTGCCT

GCTGAACAACTTCTACCCTCGGGAAGCCAAGGTGCAGTGGAAAGTGGATAAC

GCCCTGCAGTCCGGCAACTCCCAGGAAAGCGTGACCGAGCAGGACAGCAAGG

ATAGCACCTACAGCCTGTCCTCCACCCTGACCCTGTCCAAGGCCGACTACGAG

AAGCACAAGGTGTACGCCTGTGAAGTGACCCACCAGGGCCTGTCCAGCCCCGT

GACCAAGAGCTTCAACCGGGGCGAGTGTAGGGCCAAGAGGGGCGCCtaattctaga).

Amino acid sequence with annotation:

MGVKVLFALICIAVAEAEVQLVESGGGLVQPGRSLRLSCAASGFTFDDYAMHWV

	RQAPGKGLEWVSAITWNSGHIDYADSVEGRFTISRDNAKNSLYLQMNSLRAEDTA VYYCAKVSYLSTASSLDYWGQGTLVTVSSASTKGPSVFPLAPSSKSTSGGTAALG CLVKDYFPEPVTVSWNSGALTSGVHTFPAVLQSSGLYSLSSVVTVPSSSLGTQTYI CNVNHKPSNTKVDKKVEPKSCDKTHTCPPCPAPELLGGPSVFLFPPKPKDTLMISR TPEVTCVVVDVSHEDPEVKFNWYVDGVEVHNAKTKPREEQYNSTYRVVSVLTVL HQDWLNGKEYKCKVSNKALPAPIEKTISKAKGQPREPQVYTLPPSRDELTKNQVS LTCLVKGFYPSDIAVEWESNGQPENNYKTTPPVLDSDGSFFLYSKLTVDKSRWQQ GNVFSCSVMHEALHNHYTQKSLSLSPGKRAKRGSGEGRGSLLTCGDVEENPGPM GVKVLFALICIAVAEADIQMTQSPSSLSASVGDRVTITCRASQGIRNYLAWYQQKP GKAPKLLIYAASTLQSGVPSRFSGSGSGTDFTLTISSLQPEDVATYYCQRYNRAPYT FGQGTKVEIKTVAAPSVFIFPPSDEQLKSGTASVVCLLNNFYPREAKVQWKVDNA LQSGNSQESVTEQDSKDSTYSLSSTLTLSKADYEKHKVYACEVTHQGLSSPVTKSF NRGECRAKRGA Gaussia luciferase signal peptide[11] anti-hTNFα Ab heavy chain variable region[12] RAKR motif for cleavage by furine hIg gamma-1 chain constant region 2A peptide anti-hTNFα Ab light chain variable region[12] Ig kappa chain constant region	
pAS132	The NF-κB-STAT3 hybrid sensor construct. Mammalian expression vector encoding TRE-$P_{NF\text{-}\kappa B2\text{-}STAT3}$-$P_{MIN}$-driven GV16-myc expression unit (TRE-$P_{NF\text{-}\kappa B2\text{-}STAT3}$-$P_{MIN}$-GV16-myc). NF-κB-STAT3 hybrid responsive element (sequence: GGGAATTTCCGGGGACTTTCCGGGAATTTCCGGGGACTTTCCGGGAATTTCCA ACGTTCATTTCCCGTAAATCGTCGAACGTTCATTTCCCGTAAATCGTCGAACGT TCATTTCCCGTAAATCGTCGAACGTTCATTTCCCGTAAATCGTCGAACGTTCAT TTCCCGTAAATCGTCGAACGTT) was cloned into the corresponding sites (NheI/BglII) of pAS60, replacing NF-κB2 responsive element.	This work
pAS133	Synthetic gen, encoding 2A-mouse IL-10-myc tag (mIL-10). Nucleotide sequence: GGCGCCGGAAGCGGAGAGGGGAGAGGAAGTCTTCTGACCTGCGGAGACGTCG AAGAGAATCCTGGACCCATGCCCGGCAGCGCCCTGCTGTGCTGCCTGCTGCTG CTGACAGGCATGAGGATCAGCAGGGGCCAGTACAGCAGGGAGGATAACAACT	This work

	GCACCCACTTCCCCGTGGGCCAAAGCCACATGCTGCTGGAACTGAGGACCGCC TTCTCCCAGGTGAAGACCTTCTTCCAGACCAAGGACCAGCTGGACAACATCCT GCTGACCGACAGCCTGATGCAGGACTTCAAGGGCTACCTGGGCTGCCAGGCCC TGAGCGAGATGATCCAGTTCTACCTGGTGGAGGTGATGCCCCAGGCTGAGAAG CACGGCCCCGAGATCAAGGAGCACCTGAACAGCCTGGGAGAGAAGCTGAAGA CCCTGAGGATGAGGCTGAGGAGATGCCACAGGTTCCTGCCCTGCGAGAACAA GTCCAAGGCCGTGGAGCAGGTGAAGAGCGACTTCAACAAGCTGCAGGACCAG GGCGTGTACAAGGCTATGAACGAGTTCGACATCTTCATCAACTGTATCGAGGC CTACATGATGATCAAGATGAAGAGCGAGCAGAAACTCATCTCTGAAGAGGAT CTGGCGCGCTAATTCTAGA. Amino acid sequence: GAGSGEGRGSLLTCGDVEENPGPMPGSALLCCLLLLTGMRISRGQYSREDNNCTH FPVGQSHMLLELRTAFSQVKTFFQTKDQLDNILLTDSLMQDFKGYLGCQALSEMI QFYLVEVMPQAEKHGPEIKEHLNSLGEKLKTLRMRLRRCHRFLPCENKSKAVEQV KSDFNKLQDQGVYKAMNEFDIFINCIEAYMMIKMKSEQKLISEEDLAR 2A peptide Mouse IL-10-myc tag	
pAS134	Mammalian expression vector encoding TRE-UAS-P_{MIN}-driven anti-hTNFα antibody-mIL-10-myc double effector expression unit (TRE-UAS-P_{MIN}-anti-hTNFα Ab-mIL-10; DE2). 2A-Mouse IL-10 was excised from pAS133 using (KasI/XbaI) and cloned into the corresponding sites of pAS115, replacing 2A-tagBFP. MGVKVLFALICIAVAEAEVQLVESGGGLVQPGRSLRLSCAASGFTFDDYAMHWV RQAPGKGLEWVSAITWNSGHIDYADSVEGRFTISRDNAKNSLYLQMNSLRAEDTA VYYCAKVSYLSTASSLDYWGQGTLVTVSSASTKGPSVFPLAPSSKSTSGGTAALG CLVKDYFPEPVTVSWNSGALTSGVHTFPAVLQSSGLYSLSSVVTVPSSSLGTQTYI CNVNHKPSNTKVDKKVEPKSCDKTHTCPPCPAPELLGGPSVFLFPPKPKDTLMISR TPEVTCVVVDVSHEDPEVKFNWYVDGVEVHNAKTKPREEQYNSTYRVVSVLTVL HQDWLNGKEYKCKVSNKALPAPIEKTISKAKGQPREPQVYTLPPSRDELTKNQVS LTCLVKGFYPSDIAVEWESNGQPENNYKTTPPVLDSDGSFFLYSKLTVDKSRWQQ GNVFSCSVMHEALHNHYTQKSLSLSPGKRAKRGSGEGRGSLLTCGDVEENPGPM GVKVLFALICIAVAEADIQMTQSPSSLSASVGDRVTITCRASQGIRNYLAWYQQKP GKAPKLLIYAASTLQSGVPSRFSGSGSGTDFTLTISSLQPEDVATYYCQRYNRAPYT FGQGTKVEIKTVAAPSVFIFPPSDEQLKSGTASVVCLLNNFYPREAKVQWKVDNA	This work

	LQSGNSQESVTEQDSKDSTYSLSSTLTLSKADYEKHKVYACEVTHQGLSSPVTKSF NRGECRAKRGAGSGEGRGSLLTCGDVEENPGPMPGSALLCCLLLLTGMRISRGQY SREDNNCTHFPVGQSHMLLELRTAFSQVKTFFQTKDQLDNILLTDSLMQDFKGYL GCQALSEMIQFYLVEVMPQAEKHGPEIKEHLNSLGEKLKTLRMRLRRCHRFLPCE NKSKAVEQVKSDFNKLQDQGVYKAMNEFDIFINCIEAYMMIKMKSEQKLISEEDL AR Gaussia luciferase signal peptide[11] anti-hTNFα Ab heavy chain variable region[12] RAKR motif for cleavage by furine hIg gamma-1 chain constant region 2A peptide anti-hTNFα Ab light chain variable region[12] Ig kappa chain constant region mIL-10-myc tag	

Supplementary Table 2. Amount of transfected plasmids used in different experiments

Experiment/type of plate	Plasmid (detailed description in Supplementary Table 1)	Amount (ng)
Fig. 2a left/CoStar White 96-well plates (Corning)	pAS49 phRL-TK pAS48	50 5 0/0.5/1/10
Fig. 2a middle/8-well tissue culture chambers (μ-Slide 8 well, Ibidi Integrated BioDiagnostics, Martinsried München, Germany)	pAS72 pA67 pAS58 pAS75 pmCherry-C1 pAS97	80 140 30 60 25 1.5
Fig. 2b left/CoStar White 96-well plates (Corning)	pAS49 phRL-TK pSGVP pAS53	50 5 1 0/0.5/1/10/50
Fig. 2b middle/8-well tissue culture chambers (μ-Slide 8 well, Ibidi Integrated BioDiagnostics, Martinsried München, Germany)	pAS72 pA67 pAS58 pAS75 pmCherry-C1 pAS98	80 140 30 60 25 0/20
Fig. 2c/CoStar White 96-well plates (Corning)	pAS51 phRL-TK pAS58 pAS60 pAS62	50 10 0/5 0/0.5/1/10 0/0.5/1/10
Fig. 3a/CoStar White 96-well plates (Corning)	pAS51 phRL-TK pAS58 pAS60 pAS62 pAS67	45 15 5 0.5 0.5 0/5/10/25/50/75/100

Fig. 3b and Supplementary Fig. 3a/CoStar White 96-well plates (Corning)	pAS72 pAS75 pAS67 pAS58 pAS60 pAS62	45 50 75 5 0.5 0/0.5
Fig. 4a/CoStar White 96-well plates (Corning)	pAS51 phRL-TK pAS67 pAS58 pAS60 pAS62	35 15 75 5 0.5 0.5
Fig. 4b, 4c and 4d/CoStar White 96-well plates (Corning)	pAS51 phRL-TK pAS67 pAS58 pAS60 pAS62	50 15 75 5 0.5 0.5
Fig. 4e The responsiveness of the synthetic anti-inflammatory device to an inflammatory signal *in vivo*/10 cm tissue culture petri dish (TPP)	pAS72 pAS75 pAS67 pAS58 pAS60 pAS62 or pcDNA3.1 (control group)	5000 2500 3000 600 30 20 11140
Fig. 4f The responsiveness of the synthetic anti-inflammatory device in a CLP model *in vivo*/10 cm tissue culture petri dish (TPP)	pAS72 pAS75 pAS67 pAS58 pAS60	6000 1000 3500 700 30

	pAS62	20
Fig. 5b Production of therapeutic anti-inflammatory proteins *in vitro* /10 cm tissue culture petri dish (TPP)	pAS116 or pAS134 pAS75 pAS67 pAS58 pAS60 pAS62	5000 2500 3500 700 30 20
Fig. 5c Production of therapeutic anti-inflammatory proteins *in vivo* /10 cm tissue culture petri dish (TPP)	pAS116 or pAS134 pAS75 pAS67 pAS58 pAS60 pAS62	8000 2500 3500 700 30 20
Fig. 5d, 6c-e and Supplementary Fig. 6c and d Production of therapeutic anti-inflammatory proteins *in vivo* and reversibility experiments with the anti-inflammatory proteins as an output *in vivo* /10 cm tissue culture petri dish (TPP)	pAS134 pAS75 pAS67 pAS58 pAS60 pAS62	8000 1000 3500 1000 35 20
Fig. 5e/6 wells tissue culture plate (TPP) for production cell line pr CoStar White 96-well plates for reporter cell line (Corning)	Production cell line: pAS35 or pAS114 Reporter cell line: pAS40 phRL-TK	 2000 50 5
Fig. 6a, Supplementary Fig. 6a and Supplementary Fig. 7a/10 cm tissue culture petri dish (TPP)	pAS72 pAS75 pAS67 pAS58 pAS60	5000 2500 3500 600 30

	pAS62	20
Fig. 6b Restraint *in vivo* and Supplementary Fig. 7c quantification of plasmid copy drop by real-time quantitative PCR/10 cm tissue culture petri dish (TPP)	pAS72 pAS75 pAS67 pAS58 pAS60 pAS62	5000 2500 3500 1000 30 20
Fig. 7a and Supplementary Fig. 5f, right Application of the anti-inflammatory device *in vivo* in acute murine colitis/10 cm tissue culture petri dish (TPP)	pAS134 or pcDNA3.1 (control group without an effector) pAS75 pAS67 pAS58 pAS60 pAS62	8000 2500 3500 700 30 20
Supplementary Fig. 1a/CoStar White 96-well plates (Corning)	pAS36 or pAS37 phRL-TK	100 5
Supplementary Fig. 1b/CoStar White 96-well plates (Corning)	pAS37 or pAS40 phRL-TK	100 5
Supplementary Fig. 1c left/CoStar White 96-well plates (Corning)	pAS51 phRL-TK pSGVP pAS58	50 10 20 0/5/20
Supplementary Fig. 1c middle/CoStar White 96-well plates (Corning)	pAS51 phRL-TK pAS58 pAS60 pAS62	50 10 5 1 1
Supplementary Fig. 1c right/CoStar White 96-well plates (Corning)	pAS51 phRL-TK pAS58 pSGVP pAS62	50 10 5 1 0/1

Supplementary Fig. 1d left/CoStar White 96-well plates (Corning)	pAS51 phRL-TK pAS58 pAS67 pAS97 or pAS60 (to compare to) pAS98 or pAS62 (to compare to) or pAS108 (as a constitutive control)	30 10 5 75 0.5 0.5 30
Supplementary Fig. 1d right/CoStar White 96-well plates (Corning)	pAS72 pAS75 pAS58 pAS67 pAS97 or pAS60 (to compare to) pAS98 or pAS62 (to compare to) or pAS109 (as a constitutive control)	40 30 5 75 0.5 0.5 40
Supplementary Fig. 3b/8-well tissue culture chambers (μ-Slide 8 well, Ibidi Integrated BioDiagnostics, Martinsried München, Germany)	pAS72 pA67 pAS58 pAS75 pmCherry-C1 pAS97 pAS98	80 140 30 60 25 1.5 2
Supplementary Fig. 3c/8-well tissue culture chambers (μ-Slide 8 well, Ibidi Integrated BioDiagnostics, Martinsried München, Germany)	pAS72 pA67 pAS58 pAS75 pmCherry-C1 pAS97	80 140 30 60 25 0/1.5

	pAS98	0/2
Supplementary Fig. 4e/CoStar White 96-well plates (Corning)	pAS51 phRL-TK pAS58 pAS67 pAS132 pAS62 pAS123	50 15 5 75 0.5 0.5 10
Supplementary Fig. 5/CoStar White 96-well plates (Corning)	Constitutive production: pAS35 pAS114 Inducible production: pAS60 pAS62 pAS58 pAS67 pAS63 or AS113 or pAS116	 50 50 0.5 0.5 5 75 50
Supplementary Fig. 5f, left Production of therapeutic anti-inflammatory proteins *in vitro* /10 cm tissue culture petri dish (TPP)	pAS113 pAS75 pAS67 pAS58 pAS60 pAS62	5000 2500 3500 700 25 20
Supplementary Fig. 5f Production of therapeutic anti-inflammatory proteins *in vitro* and *in vivo*/10 cm tissue culture petri dish (TPP)	pAS35	25000

MATHEMATICAL MODEL

Deterministic ODE model

To predict the responsiveness of the device to stimuli and determine the optimal transfection amounts, we constructed a simple deterministic model with ordinary differential equations (ODEs) using CellDesigner 4.4 software[13]. First we constructed a state transition diagram representing the genetic circuit (Supplementary Fig. 2). Next, we characterized the state transitions with the mass action kinetic law.

The formation of a complex between a transcription factor (TF) and its corresponding response element on DNA was expressed as:

$$\frac{d[TF\text{-}DNA]}{dt} = k_a \cdot [TF] \cdot [DNA] - k_d \cdot [TF\text{-}DNA]$$

where k_a represents the on-rate constant and k_d represents the off-rate constant.

For protein (P) production, we assumed first-order kinetics:

$$\frac{d[P]}{dt} = k_s \cdot [TF\text{-}DNA]$$

and

$$\frac{d[P]}{dt} = k_l \cdot [DNA]$$

The protein production rate constant is described with k_s. Parameter k_l corresponds to leaky protein production constant that represents the basal protein synthesis from transcribed genes under the control of an uninduced minimal promoter.

Proteins are degraded to amino acids (aa) according to the first order kinetics:

$$k_{deg} \cdot [P]$$

where k_{deg} corresponds to the protein degradation constant.

We also took into account the dilution of the device's genetic components due to cell division with dilution constant k_{dil}, which corresponds to the cell doubling time.

$$k_{dil} \cdot [DNA]$$

As protein turnover is faster than the typical cell doubling ($k_{dil} < k_{deg}$), we neglected the dilution of protein moieties.

Furthermore, we assumed the amount of amino acids remained constant over the course of simulation. Thus, the model species amino acids ("aa") served as a source and a sink for protein production and degradation, respectively. Conversely, the species "lost" represented a sink for the DNA constructs lost due to the dilution by cell division. These two model species were defined as boundary conditions in the CellDesigner state transition model (see Supplementary Table 3).

Simulations

The simulations were performed using the integrated SBML ODE Solver[14]. We were particularly interested in a behavior of the device in the two limiting cases: where there was no input signal (non-stimulated), i.e. the NF-κB protein complex particle number was set to zero, and where the input signal had maximal value (stimulated). The NF-κB particle number in simulations with stimulated genetic device was set to 24 000 by taking the mean nuclear NF-κB concentration of roughly 40 nM in persistently stimulated cells[15] and estimating the volume of a cell nucleus to be $1 \cdot 10^{-12}$ L.

$$N(NF\text{-}\kappa B) = c \cdot V \cdot N_A \approx 24\,000$$

The initial quantities of genetic constructs per individual cell were estimated by taking into account the efficiency of transient transfection with polyethylenimine (PEI) and the amount of DNA·PEI complexes that are successfully trafficked to the nucleus. We estimated that 90 % of the cells ($4 \cdot 10^4$ cells per well in a 96-well plate) receive the plasmids and that 0.07 % of the initial DNA quantity reach the nucleus[16,17].

$$N(DNA) = \frac{m(DNA) \cdot 7 \cdot 10^{-4}}{M(DNA) \cdot N(cells) \cdot 0.9} \cdot N_A$$

The time t = 0 in the simulations corresponds to the transfection of the cells with DNA constructs. In time course simulations, the particle number of NF-κB was held at 24 000 for the duration of stimulation (24 h post transfection to the end of the experiment at 48 h time point post transfection), similar to the experiments with cell cultures. In parameter scan experiments, the input signal for stimulated genetic device had maximal value for the duration of the simulation (24 h).

Supplementary Table 3. List of species included in the deterministic model exported from CellDesigner 4.4 software

Class	***id***	***Name***	***Initial quantity (particle number; N)***	***Boundary condition***	***Comment***
GENE	s1	sensor	2.2	false	The sensor construct (pAS60).
GENE	s19	amplifier	2.2	false	The amplifier construct (pAS62).
GENE	s28	effector	181.8	false	The luciferase effector construct (pAS51).
GENE	s15	repressor	8.1	false	The inducible OFF-switch construct (pAS58).
GENE	s29	thresholder	425.1	false	The "thresholder" construct (pAS67).
PROTEIN	s54	GV16	0.0	false	The Gal4-VP16 transcriptional activator.
PROTEIN	s11	rtTR-KRAB*	0.0	false	The doxycycline-induced active rtTR-KRAB transcriptional repressor.
PROTEIN	s45	NF-_kappa_B	0.0	false	The NF-κB represents the input signal for the device. In the non-stimulated setting, the initial quantity was 0. Conversely, in simulations of the induced genetic device, the initial quantity was set to 24 000 (estimated from ref.[15]).

PROTEIN	s57	EFFECTOR	0.0	false	In the model, the effector protein was set to be the firefly luciferase.
PROTEIN	s49	Gal4	0.0	false	The Gal4 regulatory protein from yeast.
PROTEIN	s8	rtTR-KRAB	0.0	false	The inactive rtTR-KRAB transcriptional repressor.
COMPLEX	s43	NF-_kappa_B RE-NF-_kappa_B (sensor)	0.0	false	NF-κB in complex with its corresponding response element in the sensor construct.
COMPLEX	s40	TRE-rtTR (sensor)	0.0	false	rtTR-KRAB in complex with its corresponding response element in the sensor construct.
COMPLEX	s39	TRE-rtTR_NF-_kappa_B RE-NF-_kappa_B (sensor)	0.0	false	NF-κB and rtTR-KRAB in complex with their corresponding response elements in the sensor construct.
COMPLEX	s32	UAS-Gal4 (effector)	0.0	false	Gal4 in complex with its corresponding response element in the effector construct.
COMPLEX	s34	UAS-GV16 (effector)	0.0	false	Gal4-VP16 in complex with its corresponding response element in the effector construct.
COMPLEX	s36	TRE-rtTR_UAS-Gal4 (effector)	0.0	false	Gal4 and rtTR-KRAB in complex with their corresponding response elements in the effector construct.
COMPLEX	s42	TRE-rtTR (effector)	0.0	false	rtTR-KRAB in complex with its corresponding response element in the effector construct.
COMPLEX	s38	TRE-rtTR_UAS-GV16 (effector)	0.0	false	Gal4-VP16 and rtTR-KRAB in complex with their

					corresponding response elements in the effector construct.
COMPLEX	s31	UAS-Gal4 (amplifier)	0.0	false	Gal4 in complex with its corresponding response element in the amplifier construct.
COMPLEX	s33	UAS-GV16 (amplifier)	0.0	false	Gal4 in complex with its corresponding response element in the amplifier construct.
COMPLEX	s35	TRE-rtTR_UAS-Gal4 (amplifier)	0.0	false	Gal4 and rtTR-KRAB in complex with their corresponding response elements in the amplifier construct.
COMPLEX	s41	TRE-rtTR (amplifier)	0.0	false	rtTR-KRAB in complex with its corresponding response element in the ampllifier construct.
COMPLEX	s37	TRE-rtTR_UAS-GV16 (amplifier)	0.0	false	Gal4-VP16 and rtTR-KRAB in complex with their corresponding response elements in the amplifier construct.
SIMPLE_MOLECULE	s58	Dox	0.0	true	Doxycycline (OFF-switch inducer) moiety.
DEGRADED	s30	aa	0.0	true	Amino acids (protein source and sink in the model).
DEGRADED	s16	lost	0.0	true	Lost DNA constructs due to dilution through cell division (sink in the model).

Supplementary Table 4. List of parameters included in the deterministic model exported from CellDesigner 4.4 software

id	*Name*	*Description*	*Value*	*Units*	*Comment*
ka_GV16	k_a^{GV16}	Gal4-VP16 - DNA on-rate binding constant.	$1.66 \cdot 10^{-6}$	$N^{-1} \cdot s^{-1}$	Value was calculated from $1 \cdot 10^6$ $M^{-1} \cdot s^{-1}$ (estimated from ref.[18]; $K_D \approx 10$ nM).
kd_GV16	k_d^{GV16}	Gal4-VP16 - DNA off-rate constant.	0.01	s^{-1}	Value was estimated from ref.[19].
k_l	k_l	Leaky protein production rate.	0.00125	s^{-1}	Estimated value represents 0.5 % of the maximal protein production rate.
k_deg	k_{deg}	Average protein degradation rate.	$2.79045 \cdot 10^{-5}$	s^{-1}	Value was calculated from estimated average protein half life in humans (6.9 h)[20].
ka_NFkB	$k_a^{NFκB}$	NF-κB - DNA on-rate binding constant.	$1.66 \cdot 10^{-6}$	$N^{-1} \cdot s^{-1}$	Value was calculated from $1 \cdot 10^{-6}$ $M^{-1} \cdot s^{-1}$[19].
kd_NFkB	$k_d^{NFκB}$	NF-κB - DNA off-rate constant.	0.01	s^{-1}	Value was estimated from ref.[18].
k_s	k_s	Protein production rate.	0.25	s^{-1}	Estimated.
k_dil	k_{dil}	Dilution rate.	$8.02254 \cdot 10^{-6}$	s^{-1}	Calculated from estimated cell generation time of 24 h.
k_dox	k^{dox}	Doxycycline – rtTR-KRAB association constant.	$1.66 \cdot 10^{-6}$	$N^{-1} \cdot s^{-1}$	Calculated from $1 \cdot 10^6$ $M^{-1} \cdot s^{-1}$ (estimated from ref.[21]).
ka_rtTR	k_a^{rtTR}	rtTR-KRAB - DNA on-rate binding constant.	$1.66 \cdot 10^{-6}$	$N^{-1} \cdot s^{-1}$	Estimated.
kd_rtTR	k_d^{rtTR}	rtTR-KRAB - DNA off-rate constant.	0.01	s^{-1}	Estimated.
k_deg_luc	k_{deg}^{luc}	Firefly luciferase degradation rate.	$9.62704 \cdot 10^{-5}$	s^{-1}	Value was calculated from luciferase half life in HEK 293T cells (2 h)[22].
k_deg_gal4	k_{deg}^{gal4}	Gal4 degradation rate.	$1.15525 \cdot 10^{-4}$	s^{-1}	Value was calculated from Gal4 half life in HeLa cells (100 min)[23].
k_deg_gv16	k_{deg}^{gv16}	Gal4-VP16 degradation rate.	$1.54033 \cdot 10^{-4}$	s^{-1}	Value was calculated from Gal4-VP16 half life in HeLa cells (75 min)[23].

Supplementary Table 5. List of reactions included in the deterministic model exported from CellDesigner 4.4 software

Type	*id*	*Reversible*	*Reaction*	*Trigger*	*Math*	*Comment*
HETERODIMER_ASSOCIATION	re1	true	$s45 + s1 \leftrightharpoons s43$		$\frac{d[s43]}{dt} = s45 \cdot s1 \cdot ka\_NFkB - s43 \cdot kd\_NFkB$	Binding and dissociation of NF-κB complex to its corresponding response element on the sensor construct.
STATE_TRANSITION	re2	false	$s30 \rightarrow s54$	s43	$\frac{d[s54]}{dt} = s43 \cdot k\_s$	Production of Gal4-VP16 from amino acids, triggered by NF-κB-induced transcription of the sensor construct expression unit.
STATE_TRANSITION	re3	false	$s30 \rightarrow s8$	s15	$\frac{d[s30]}{dt} = s15 \cdot k\_s$	Production of inactive rtTR-KRAB from amino acids, triggered by constitutive transcription from the repressor construct expression unit.
HETERODIMER_ASSOCIATION	re4	true	$s54 + s19 \rightleftharpoons s33$		$\frac{d[s33]}{dt} = s54 \cdot s19 \cdot ka\_GV16 - s33 \cdot kd\_GV16$	Binding and dissociation of Gal4-VP16 to its corresponding response

						element on the amplifier construct.
STATE_TRANSITION	re5	false	$s8 \rightarrow s30$		$\frac{d[s30]}{dt} = s8 \cdot k\_deg$	Inactive rtTR-KRAB degradation.
HETERODIMER_ASSOCIATION	re6	true	$s54 + s28 \rightleftharpoons s34$		$\frac{d[s34]}{dt} = s54 \cdot s28 \cdot ka\_GV16 - s34 \cdot kd\_GV16$	Binding and dissociation of Gal4-VP16 to its corresponding response element on the effector construct.
STATE_TRANSITION	re7	false	$s30 \rightarrow s57$	s34	$\frac{d[s57]}{dt} = s34 \cdot k\_s$	Production of luciferase reporter from amino acids, triggered by Gal4-VP16-induced transcription of the effector construct expression unit.
STATE_TRANSITION	re8	false	$s54 \rightarrow s30$		$\frac{d[s30]}{dt} = s54 \cdot k\_deg\_gv16$	Gal4-VP16 degradation to amino acids.
STATE_TRANSITION	re9	false	$s30 \rightarrow s49$	s29	$\frac{d[s49]}{dt} = s29 \cdot k\_s \cdot 0.01$	Production of Gal4 from amino acids, triggered by constitutive transcription from the “thresholder” construct

						expression unit. The production rate was set to 1 % of the estimated maximal protein production rate (k_s).
HETERODIMER_ASSOCIATION	re10	true	$s49 + s19 \rightleftharpoons s31$		$\frac{d[s31]}{dt} = s49 \cdot s19 \cdot ka\_GV16 - s31 \cdot kd\_GV16$	Binding and dissociation of Gal4 to its corresponding response element on the amplifier construct.
HETERODIMER_ASSOCIATION	re11	true	$s49 + s28 \rightleftharpoons s32$		$\frac{d[s32]}{dt} = s49 \cdot s28 \cdot ka\_GV16 - s32 \cdot kd\_GV16$	Binding and dissociation of Gal4 to its corresponding response element on the effector construct.
STATE_TRANSITION	re12	false	$s49 \rightarrow s30$		$\frac{d[s30]}{dt} = s49 \cdot k\_deg\_gal4$	Gal4 degradation to amino acids.
STATE_TRANSITION	re13	false	$s30 \rightarrow s54$	s1	$\frac{d[s54]}{dt} = s1 \cdot k\_l$	Production of Gal4-VP16 from amino acids, triggered by leaky transcription of the sensor construct expression unit.
STATE_TRANSITION	re14	false	$s30 \rightarrow s54$	s33	$\frac{d[s54]}{dt} = s33 \cdot k\_s$	Production of

						Gal4-VP16 from amino acids, triggered by Gal4-VP16-induced transcription of the amplifier construct expression unit.
STATE_TRANSITION	re15	false	s30 → s54	s19	$\frac{d[s54]}{dt} = s19 \cdot k\_l$	Production of Gal4-VP16 from amino acids, triggered by leaky transcription of the amplifier construct expression unit.
STATE_TRANSITION	re16	false	s30 → s57	s28	$\frac{d[s57]}{dt} = s28 \cdot k\_l$	Production of luciferase reporter from amino acids, triggered by leaky transcription of the effector construct expression unit.
STATE_TRANSITION	re17	false	s57 → s30		$\frac{d[s30]}{dt} = s57 \cdot k\_deg\_luc$	Luciferase reporter degradation to amino acids.
STATE_TRANSITION	re18	false	s30 → s54	s31	$\frac{d[s54]}{dt} = s31 \cdot k\_l \cdot 0.01$	Production of Gal4-VP16 from amino acids, triggered by leaky

						transcription of the Gal4-bound amplifier construct expression unit. The repressed leaky production rate was set to 1 % of the unrepressed leaky production rate.
STATE_TRANSITION	re19	false	s30 → s57	s32	$\frac{d[s57]}{dt} = s32 \cdot k\_l \cdot 0.01$	Production of luciferase effector from amino acids, triggered by leaky transcription of the Gal4-bound effector construct expression unit. The repressed leaky production rate was set to 1 % of the unrepressed leaky production rate.
STATE_TRANSITION	re20	false	s1 → s16		$\frac{d[s16]}{dt} = s1 \cdot k\_dil$	Dilution of the sensor construct due to cell division.
STATE_TRANSITION	re21	false	s29 → s16		$\frac{d[s16]}{dt} = s29 \cdot k\_dil$	Dilution of the “thresholder” construct due to

						cell division.
STATE_TRANSITION	re22	false	$s15 \rightarrow s16$		$\frac{d[s16]}{dt} = s15 \cdot k\_dil$	Dilution of the repressor construct due to cell division.
STATE_TRANSITION	re23	false	$s19 \rightarrow s16$		$\frac{d[s16]}{dt} = s19 \cdot k\_dil$	Dilution of the amplifier construct due to cell division.
STATE_TRANSITION	re24	false	$s28 \rightarrow s16$		$\frac{d[s16]}{dt} = s28 \cdot k\_dil$	Dilution of the effector construct due to cell division.
STATE_TRANSITION	re25	false	$s8 \rightarrow s11$	s58	$\frac{d[s11]}{dt} = s8 \cdot s58 \cdot k\_dox$	Binding of doxycycline to an inactive rtTR-KRAB, producing an active rtTR-KRAB.
HETERODIMER_ASSOCIATION	re26	true	$s11 + s34 \rightleftharpoons s38$		$\frac{d[s38]}{dt} = s11 \cdot s34 \cdot ka\_rtTR - s38 \cdot kd\_rtTR$	Binding and dissociation of rtTR-KRAB to its corresponding response element on the Gal4-VP16-bound effector construct.
HETERODIMER_ASSOCIATION	re27	true	$s11 + s28 \rightleftharpoons s42$		$\frac{d[s42]}{dt} = s11 \cdot s28 \cdot ka\_rtTR - s42 \cdot kd\_rtTR$	Binding and dissociation of rtTR-KRAB to its corresponding response element on the

						effector construct.
HETERODIMER_ASSOCIATION	re28	true	$s11 + s32 \rightleftharpoons s36$		$\frac{d[s36]}{dt} = s11 \cdot s32 \cdot ka\_rtTR - s36 \cdot kd\_rtTR$	Binding and dissociation of rtTR-KRAB to its corresponding response element on the Gal4-bound effector construct.
HETERODIMER_ASSOCIATION	re29	true	$s11 + s33 \rightleftharpoons s37$		$\frac{d[s37]}{dt} = s11 \cdot s33 \cdot ka\_rtTR - s37 \cdot kd\_rtTR$	Binding and dissociation of rtTR-KRAB to its corresponding response element on the Gal4-VP16-bound amplifier construct.
HETERODIMER_ASSOCIATION	re30	true	$s11 + s19 \rightleftharpoons s41$		$\frac{d[s41]}{dt} = s11 \cdot s19 \cdot ka\_rtTR - s41 \cdot kd\_rtTR$	Binding and dissociation of rtTR-KRAB to its corresponding response element on the amplifier construct.
HETERODIMER_ASSOCIATION	re31	true	$s11 + s31 \rightleftharpoons s35$		$\frac{d[s35]}{dt} = s11 \cdot s31 \cdot ka\_rtTR - s35 \cdot kd\_rtTR$	Binding and dissociation of rtTR-KRAB to its corresponding response

						element on the Gal4-bound amplifier construct.
HETERODIMER_ASSOCIATION	re32	true	$s11 + s1 \rightleftharpoons s40$		$\frac{d[s40]}{dt} = s11 \cdot s1 \cdot ka\_rtTR - s40 \cdot kd\_rtTR$	Binding and dissociation of rtTR-KRAB to its corresponding response element on the sensor construct.
HETERODIMER_ASSOCIATION	re33	true	$s11 + s43 \rightleftharpoons s39$		$\frac{d[s39]}{dt} = s11 \cdot s43 \cdot ka\_rtTR - s39 \cdot kd\_rtTR$	Binding and dissociation of rtTR-KRAB to its corresponding response element on the NF-κB-bound sensor construct.
STATE_TRANSITION	re34	false	$s43 \rightarrow s16$		$\frac{d[s16]}{dt} = s43 \cdot k\_dil$	Dilution of the NF-κB-bound sensor construct due to cell division.
STATE_TRANSITION	re35	false	$s40 \rightarrow s16$		$\frac{d[s16]}{dt} = s40 \cdot k\_dil$	Dilution of the rtTR-KRAB-bound sensor construct due to cell division.
STATE_TRANSITION	re36	false	$s39 \rightarrow s16$		$\frac{d[s16]}{dt} = s39 \cdot k\_dil$	Dilution of the NF-κB and rtTR-KRAB-bound sensor construct due to cell division.

STATE_TRANSITION	re39	false	$s31 \rightarrow s16$		$\frac{d[s16]}{dt} = s31 \cdot k\_dil$	Dilution of the Gal4-bound amplifier construct due to cell division.
STATE_TRANSITION	re40	false	$s33 \rightarrow s16$		$\frac{d[s16]}{dt} = s33 \cdot k\_dil$	Dilution of the Gal4-VP16-bound amplifier construct due to cell division.
STATE_TRANSITION	re42	false	$s11 \rightarrow s30$		$\frac{d[s30]}{dt} = s11 \cdot k\_deg$	Active rtTR-KRAB degradation.
STATE_TRANSITION	re44	false	$s35 \rightarrow s16$		$\frac{d[s16]}{dt} = s35 \cdot k\_dil$	Dilution of the Gal4 and rtTR-KRAB-bound amplifier construct due to cell division.
STATE_TRANSITION	re45	false	$s41 \rightarrow s16$		$\frac{d[s16]}{dt} = s41 \cdot k\_dil$	Dilution of the rtTR-KRAB-bound amplifier construct due to cell division.
STATE_TRANSITION	re46	false	$s37 \rightarrow s16$		$\frac{d[s16]}{dt} = s37 \cdot k\_dil$	Dilution of the Gal4-VP16 and rtTR-KRAB-bound amplifier construct due to cell division.
STATE_TRANSITION	re47	false	$s32 \rightarrow s16$		$\frac{d[s16]}{dt} = s32 \cdot k\_dil$	Dilution of the Gal4-bound effector construct due to cell division.
STATE_TRANSITION	re48	false	$s34 \rightarrow s16$		$\frac{d[s16]}{dt} = s34 \cdot k\_dil$	Dilution of the Gal4-VP16-

						bound amplifier construct due to cell division.
STATE_TRANSITION	re49	false	s36 → s16		$\frac{d[s16]}{dt} = s36 \cdot k\_dil$	Dilution of the Gal4 and rtTR-KRAB-bound effector construct due to cell division.
STATE_TRANSITION	re50	false	s42 → s16		$\frac{d[s16]}{dt} = s42 \cdot k\_dil$	Dilution of the rtTR-KRAB-bound effector construct due to cell division.
STATE_TRANSITION	re51	false	s38 → s16		$\frac{d[s16]}{dt} = s38 \cdot k\_dil$	Dilution of the Gal4-VP16 and rtTR-KRAB-bound effector construct due to cell division.

SUPPLEMENTARY REFERENCES

1. King, GA, Daugulis, AJ, Faulkner, P and Goosen, MFA. (1987). Alginate-Polylysine Microcapsules of Controlled Membrane Molecular Weight Cutoff for Mammalian Cell Culture Engineering. *Biotechnol. Prog.* **3**: 231–240.
2. Dubrot, J, Portero, A, Orive, G, Hernández, RM, Palazón, A, Rouzaut, A, *et al.* (2010). Delivery of immunostimulatory monoclonal antibodies by encapsulated hybridoma cells. *Cancer Immunol. Immunother.* **59**: 1621–1631.
3. Wirtz, S, Neufert, C, Weigmann, B and Neurath, MF (2007). Chemically induced mouse models of intestinal inflammation. *Nat. Protoc.* **2**: 541–546.
4. Fussenegger, M, Morris, RP, Fux, C, Rimann, M, von Stockar, B, Thompson, CJ, *et al.* (2000). Streptogramin-based gene regulation systems for mammalian cells. *Nat. Biotechnol.* **18**: 1203–1208.
5. Sadowski, I, Ma, J, Triezenberg, S and Ptashne, M (1988). GAL4-VP16 unusualy potent transcription activator. *Nature* **335**: 563–564.
6. Szulc, J, Wiznerowicz, M, Sauvain, M, Trono, D and Aebischer, P (2006). A versatile tool for conditional gene expression and knockdown. *Nat. Methods* **3**.
7. Fussenegger, M, Mazur, X and Bailey, JE (1997). A Novel Cytostatic Process Enhances the Ovary Cells. *Biotechnol Bioeng*. **20**:927-939.
8. Lebar, T, Straz, M, Bezeljak, U, Golob, A, Jerala, M, Kadunc, L, *et al.* (2014). A bistable genetic switch based on designable DNA-binding domains. **29**: 5007
9. Gibson, DG, Young, L, Chuang, R-Y, Venter, JC, Hutchison, CA and Smith, HO (2009). Enzymatic assembly of DNA molecules up to several hundred kilobases. *Nat. Methods* **6**: 343–345.
10. Kim, JH, Lee, SR, Li, LH, Park, HJ, Park, JH, Lee, KY, *et al.* (2011). High cleavage efficiency of a 2A peptide derived from porcine teschovirus-1 in human cell lines, zebrafish and mice. *PLoS One* **6**: 1–8.
11. Stern, B, Olsen, LC, Tröße, C, Ravneberg, H and Pryme, IF (2007). Improving mammalian cell factories : The selection of signal peptide has a major impact on recombinant protein synthesis and secretion in mammalian cells. *Trends Cell Mol. Biol.* **2**: 1–17.
12. Abbott Biotechnology Ltd. Human antibodies that bind human TNFα. US Patent 6,090,382 filed 9 Feb. 1996, and issued 18 Jul. 2000.
13. Funahashi, A, Morohashi, M, Kitano, H and Tanimura, N (2003). CellDesigner: a process diagram editor for gene-regulatory and biochemical networks. *Biosilico* **1**: 159–162.
14. Machné, R, Finney, A, Müller, S, Lu, J, Widder, S and Flamm, C (2006). The SBML ODE Solver Library: A native API for symbolic and fast numerical analysis of reaction networks. *Bioinformatics* **22**: 1406–1407.
15. Hoffmann, A, Levchenko, A, Scott, ML and Baltimore, D (2002). The IkappaB-NF-kappaB signaling module: temporal control and selective gene activation. *Science* **298**: 1241–1245.
16. Kichler, A, Leborgne, C, Coeytaux, E and Danos, O (2001). Polyethylenimine-mediated gene delivery: A mechanistic study. *J. Gene Med.* **3**: 135–144.

17. Pollard, H, Remy, JS, Loussouarn, G, Demolombe, S, Behr, JP and Escande, D (1998). Polyethylenimine but not cationic lipids promotes transgene delivery to the nucleus in mammalian cells. *J. Biol. Chem.* **273**: 7507–7511.

18. Hong, M, Fitzgerald, MX, Harper, S, Luo, C, Speicher, DW and Marmorstein, R (2008). Structural Basis for Dimerization in DNA Recognition by Gal4. *Structure* **16**: 1019–1026.

19. Bergqvist, S, Alverdi, V, Mengel, B, Hoffmann, A, Ghosh, G and Komives, E a (2009). Kinetic enhancement of NF-kB - DNA dissociation by IkBa. **2009**: 1–6.

20. Eden, E, Geva-Zatorsky, N, Issaeva, I, Cohen, A, Dekel, E, Danon, T, *et al.* (2011). Proteome half-life dynamics in living human cells. *Science* **331**: 764–768.

21. Sotiropoulos, V and Kaznessis, YN (2007). Synthetic tetracycline-inducible regulatory networks: computer-aided design of dynamic phenotypes. *BMC Syst. Biol.* **1**: 7.

22. Ignowski, JM and Schaffer, D V. (2004). Kinetic analysis and modeling of firefly luciferase as a quantitative reporter gene in live mammalian cells. *Biotechnol. Bioeng.* **86**: 827–834.

23. Salghetti, SE, Muratani, M, Wijnen, H, Futcher, B and Tansey, WP (2000). Functional overlap of sequences that activate transcription and signal ubiquitin-mediated proteolysis. *Proc. Natl. Acad. Sci. U. S. A.* **97**: 3118–3123.